Vaccine 42 (2024) 126394

Contents lists available at ScienceDirect

Vaccine

journal homepage: www.elsevier.com/locate/vaccine

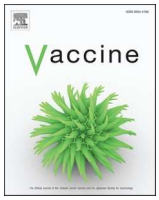

SpiN-Tec: A T cell-based recombinant vaccine that is safe, immunogenic, and shows high efficacy in experimental models challenged with SARS-CoV-2 variants of concern

Natália S. Hojo-Souza [a,b,1], Júlia T. de Castro [a,b,c,1], Graziella G. Rivelli [a], Patrick O. Azevedo [a,b], Emiliano R. Oliveira [b], Lídia P. Faustino [a,b], Natália Salazar [a], Flávia F. Bagno [a], Alex F. Carvalho [a], Bruna Rattis [c], Karine L. Lourenço [a], Isabela P. Gomes [a], Bruna R.D. Assis [a,g], Mariela Piccin [c], Flávio G. Fonseca [a,d], Edison Durigon [e], João S. Silva [c], Renan P. de Souza [a,f], Gisele A.C. Goulart [a,g], Helton Santiago [a,h], Ana Paula S. Fernandes [a,g], Santuza R. Teixeira [a,h], Ricardo T. Gazzinelli [a,b,h,*]

[a] Centro de Tecnologia de Vacinas, Universidade Federal de Minas Gerais, Brazil
[b] Instituto René Rachou, Fundação Oswaldo Cruz-Minas, Brazil
[c] Plataforma Bi-Institucional de Pesquisa em Medicina Translacional, Fundação Oswaldo Cruz, Faculdade de Medicina de Ribeirão Preto, Universidade de São Paulo, Brazil
[d] Departamento de Microbiologia, Universidade Federal de Minas Gerais, Brazil
[e] Instituto de Ciências Biológicas, Universidade de São Paulo, Brazil
[f] Departamento de Genética, Ecologia e Evolução, Universidade Federal de Minas Gerais, Brazil
[g] Faculdade de Farmácia, Universidade Federal de Minas Gerais, Brazil
[h] Departamento de Bioquímica e Imunologia, Universidade Federal de Minas Gerais, Brazil

ARTICLE INFO

Keywords:
Vaccine
COVID-19
SARS-CoV-2

ABSTRACT

The emergence of new SARS-CoV-2 variants of concern associated with waning immunity induced by natural infection or vaccines currently in use suggests that the COVID-19 pandemic will become endemic. Investing in new booster vaccines using different platforms is a promising way to enhance protection and keep the disease under control. Here, we evaluated the immunogenicity, efficacy, and safety of the SpiN-Tec vaccine, based on a chimeric recombinant protein (SpiN) adjuvanted with CTVad1 (MF59-based adjuvant), aiming at boosting immunity against variants of concern of SARS-CoV-2. Immunization of K18-hACE-2 transgenic mice and hamsters induced high antibody titers and cellular immune response to the SpiN protein as well as to its components, RBD and N proteins. Importantly in a heterologous prime/boost protocol with a COVID-19 vaccine approved for emergency use (ChAdOx1), SpiN-Tec enhanced the level of circulation neutralizing antibodies (nAb). In addition to protection against the Wuhan isolate, protection against the Delta and Omicron variants was also observed as shown by reduced viral load and lung pathology. Toxicity and safety tests performed in rats demonstrated that the SpiN-Tec vaccine was safe and, based on these results, the SpiN-Tec phase I/II clinical trial was approved.

1. Introduction

The continuous emergence of new SARS-CoV-2 variants/subvariants that escape the immunity provided by the vaccines in use has made COVID-19 an endemic disease. Updating vaccines according to the circulating variant/subvariant or developing new ones through different platforms is the best strategy, given that during the pandemic, vaccines approved for emergency use were able to reduce severe cases, hospitalizations, and deaths. The development of safe and effective vaccines using different platforms, capable of inducing a diversified immune response is highly recommended, particularly if they are associated with relatively easy low-cost production and are stable at refrigerator

* Corresponding author at: Centro de Tecnologia de Vacinas, Instituto René Rachou, Fundação Oswaldo Cruz-Minas, Universidade Federal de Minas Gerais, Brazil.
E-mail address: ricardo.gazzinelli@fiocruz.br (R.T. Gazzinelli).
[1] These authors contributed equally to this work

https://doi.org/10.1016/j.vaccine.2024.126394
Received 12 December 2023; Received in revised form 11 September 2024; Accepted 21 September 2024
Available online 4 October 2024

temperature storage conditions. Considering that most vaccines against COVID-19 are based on the SARS-CoV-2 Spike protein, which is susceptible to mutations favoring the emergence of variants of concern (VOCs), current vaccines may not provide long-lasting robust protection. Therefore, the inclusion of other SARS-CoV-2 antigens such as the nucleocapsid (N) protein in the process of development of new COVID-19 vaccines that can be used as booster vaccines has been suggested, as N protein is widely conserved and may provide strong immunity to novel viral variants [1].

We have developed a vaccine based on a chimeric antigen (SpiN) comprising the receptor binding domain (RBD) from the Spike and the full-length sequence of the N protein from SARS-CoV-2. Mice immunization with SpiN adjuvanted with Poly ICLC induced a strong IFN-γ response by T cells and high levels of antibodies. Syrian hamsters and human Angiotensin Convertase Enzyme-2-transgenic (K18-hACE-2) mice showed strong resistance to the infection with the Wuhan SARS-CoV-2 and this protection is mediated by $CD4^+$ and $CD8^+$ T cells. Furthermore, immunization with SpiN also protected K18-hACE-2 mice against infection with the Delta and Omicron SARS-CoV-2 isolates [2].

Emerging data are increasingly consolidating the involvement of $CD4^+$ and $CD8^+$ T cells in protection against SARS-CoV-2. Studies on immune responses to the mRNA-based vaccine in use have shown that vaccinated individuals have robust anti-S and anti-RBD antibody responses, which decline over the months post-vaccination but can be restored with booster doses. Spike-specific $CD4^+$ and $CD8^+$ T cells are also induced by mRNA vaccines. The $CD4^+$ and $CD8^+$ T cells are detectable months after vaccination [3] and cross-react to SARS-CoV-2 variants [4]. Several studies have demonstrated that despite declining neutralizing antibodies (nAb) levels, individuals immunized with a Spike-based vaccine containing sequences of the Wuhan SARS-CoV-2 as well as COVID-19 convalescents show a robust cross-reactivity of $CD4^+$ and $CD8^+$ T cells against VOCs, suggesting that protection against severe disease is mediated by T cells [3,5–8]. Other studies show that vaccines combining Spike and nucleocapsid proteins improve control of a SARS-CoV-2 infection by increasing T cell responses [9,10]. Considering that heterologous booster vaccine schedules for COVID-19 resulted in increased protection against reinfection and severe disease compared to a homologous booster protocol [11,12], the development of different vaccine formulations, especially those capable of inducing T cell responses, is a relevant strategy to control infection.

Despite the promising results obtained with SpiN chimeric protein adjuvanted with Poly ICLC, this adjuvant is not approved for human use, so we decided to switch to an MF59-based adjuvant, aiming for a formulation that can meet regulatory requirements for products for human use. Here, we evaluated the immunogenicity, efficacy, and safety of SpiN-Tec, the SpiN recombinant chimeric protein adjuvanted with the MF59-based adjuvant named CTVad, in a preclinical study using Syrian hamsters and K18-hACE-2 mice. The SpiN-Tec vaccine is aimed to be used as a booster vaccine that is capable of protecting against distinct variants of concern. Our findings indicate that using a heterologous prime-boost protocol, SpiN-Tec induces high levels of IFN-γ produced by T cells, as well as high levels of circulating nAbs. Importantly, an extensive characterization and stability study of the adjuvant produced in our laboratories (CTVad1) was performed as well as in vivo experiments with the SpiN-CTVad1 adjuvanted vaccine (named SpiN-Tec). All critical process parameters, both for the CTVad1 production and the formulation of SpiN-Tec were met including critical quality attributes required for approval by Brazilian regulatory agencies [13].

2. Material and methods

2.1. Ethical statement

The experiments were carried out following the principles of conduct of the Brazilian Guide to Practices for the Care and Use of Animals for Scientific and Didactic Purposes of Conselho Nacional de Controle de Experimentação Animal (CONCEA) (http://www.sbcal.org.br). The experimental protocols used were previously approved by the Committee on Ethics in the Use of Animals (CEUA) of Fundação Oswaldo Cruz (CEUA protocol LW25/20), Universidade de São Paulo (CEUA protocol 105/2020) and Centro de Inovação e Ensaios Pré-Clínicos (CIEnP) (CEUA protocol 308/00).

2.2. Experimental animals

Immunogenicity assays were carried out with female C57BL/6 mice, 6–10 weeks old, from Center for Laboratory Animal Facilities of the Universidade Federal de Minas Gerais (CEBIO-UFMG). Human angiotensin-converting enzyme 2 transgenic mice (K18-hACE2), were bred at the Fiocruz-Minas Laboratory Animal Facilities after purchasing matrices from The Jackson Laboratory. Knockout mice for B cells and transgenic for angiotensin-converting enzyme 2 (K18-hACE2/B-KO), were bred at Fiocruz-Minas animal facilities. K18-hACE2 and K18-hACE2/B-KO mice, 6–10 weeks old, were used as a model of severe COVID-19. Golden Syrian hamsters, 6–10 weeks old, from FIOCRUZ-Minas Animal Facilities, were used as a model of moderate COVID-19. Sprague Dawley rats, 6–10 weeks old, were used in the safety and toxicity tests at CIEnP.

2.3. Virus and Cells

The ancestral strain of SARS-CoV-2 (isolated BRA/SP02/2020), Delta variant (EPI_ISL_2965577) and Omicron (EPI_ISL_7699344) used in the challenge and PRNT50 assays were isolated from clinical samples from Brazilian patients with COVID-19. All virus used were sequenced to confirm the strain/variant. VERO E6 cells (ATCC CRL-1586) were incubated in the presence of the virus for 1 h under agitation. After this period, the cells were incubated for 72 h in DMEM medium, supplemented with 2 % fetal bovine serum (Sigma) and 1 % of penicillin/streptomycin (Sigma). The cells were removed with the aid of a cell scraper and the suspension was centrifuged for viral clarification. The viral stocks obtained were serially diluted in a ratio of [1:10 to 1:1,000,000 (v/v)] for viral titration using Vero E6 cells in 48-well plates at a ratio of 5×10^4 cells/well.

2.4. SpiN protein production and SpiN-Tec vaccine

The SpiN protein design was performed by epitope prediction through the Immune Epitope Database (IEDB) platform for HLA-ABC and MHC class I analysis and NetMHCII for HLA-DR and MHC class II considering the sequences of Spike (6VSB https://doi.org/10.2210/pdb6VSB/pdb) and Nucleocapsid (7SD4_1 https://doi.org/10.2210/pdb7SD4/pdb) proteins from Wuhan isolate. Gene sequences encoding the chimeric SpiN protein were codon-optimized for expression in *E. coli* and synthesized by GenScript using the pET24 expression vector. *E. coli* Shuffle bacteria were transformed using the pET24_SpiN plasmid and grown in LB medium supplemented with kanamycin (50 μg/mL) at 37 °C until reaching an OD600 from 0.4 to 0.6. Protein expression was induced by adding IPTG at a final concentration of 0.5 mM for a period of 15 h at 37 °C. SpiN protein was purified from insoluble fractions by adding 8 M of urea and submitted to anion exchange with Hitrap Q XL column (GE HealthCare), followed by a cation exchange chromatography with Hitrap SP HP column (GE HealthCare). The purified SpiN protein was diluted in sodium phosphate buffer (100 mM), urea (100 mM), sodium chloride (150 mM), glycerol (10 %), and water to a final concentration of 0.40 mg/mL, pH = 7.5, constituting the active pharmaceutical ingredient (API) of SpiN-Tec vaccine. The technology for SpiN protein production was developed by Centro de Tecnologia de Vacinas (CT-Vacinas – UFMG) and transferred to the University of Nebraska, where the API was produced under good laboratory practice (GLP). Finally, the API was associated with the nanoemulsion CTVad1 (adjuvant) produced by CT-Vacinas, generating the SpiN-Tec vaccine.

2.5. Immunization and challenge experiments

Two lots of SpiN-Tec were used for immunization: 100 μg/mL (Lot: 21/1880) and 200 μg/mL (Lot: 21/1879). All experimental animals were immunized with two doses of SpiN-Tec intramuscularly 21 days apart. C57BL/6 and K18-hACE2 mice were immunized with 10 μg or 20 μg of SpiN (100 μL/dose), hamsters were immunized with 25 μg or 50 μg of SpiN (250 μL/dose) and rats were immunized with 50 μg or 100 μg of SpiN (500 μL/dose) in the tibial muscle. The control groups received an equivalent volume of CTVad + Vehicle. Thirty days after the booster dose, K18-hACE2 mice were challenged intranasally with 5×10^4 PFU of the ancestral SARS-CoV-2 (Wuhan) or 2.5×10^4 PFU of the Omicron variant. Hamsters were challenged with 10^5 PFU for all variants used (Wuhan, Delta, and Omicron). For heterologous prime/boost, K18-hACE2 mice were immunized with PBS or ChAdOx1 (1×10^{10} PV; Lot: L218VCD245W – Fiocruz/Bio-Manguinhos) and boosted with SpiN-Tec (10 μg; Lot: 21/1880) or ChAdOx1.

2.6. Detection of mouse, hamster, and rat antigen-specific antibodies

Total IgG and subclasses were quantified by ELISA in 96-well plates (Nunc Maxisorp, Thermo Fisher Scientific) coated with 4 μg/mL of RBD, N, SpiN (produced at CT-Vacinas) or RBD Omicron (Fapon Biotech) recombinant protein diluted in carbonate buffer and incubated overnight at 4 °C. The next day, plates were washed and blocked for 2 h with PBS containing 2 % BSA (Sigma) at 37 °C. Serial sera sample dilutions in PBS-BSA 2 % from 1:100 to 1:625,000 (v/v) were incubated for 1 h at 37 °C. The plates were washed and incubated for 2 h at 37 °C with anti-mouse total IgG, IgG1 or IgG2c, anti-hamster total IgG, IgG1 or IgG2/IgG3 or anti-rat total IgG, IgG1 or IgG2b, conjugated with streptavidin-HRP (Southern Biotech), all diluted at a ratio of 1:5,000 (v/v). After successive washes, the plates were incubated with the substrate solution One-Step TMB (Scienco), for 20 min protected from light at room temperature. The reaction was stopped by adding 2 N H_2SO_4 (Sigma). Plate reading was performed at 450 nm in the Multiskan GO (Thermo Scientific). The evaluation of the humoral immune response was carried out through the quantification of antibody titers, calculated by the inverse of the maximum dilution at which the absorbance value was higher than the cutoff (average of the control group at dilution 1:100 plus 3 standard deviations) [14].

2.7. Plaque Reduction Neutralization Test (PRNT)

Vero E6 cells were cultured in 48-well plates using Dulbecco's Modified Eagle's Medium (DMEM) supplemented with 1 % penicillin/streptomycin and 10 % fetal bovine serum. Sera samples were inactivated at 56 °C, serially diluted in DMEM [1:20 to 1:625,000 (v/v)], mixed with 100 PFU of SARS-CoV-2 (Wuhan) or Omicron variant, and incubated at 37 °C for 1 h. To determine the viral neutralizing capacity of sera antibodies from immunized animals, the virus suspension added to sera was incubated for 1 h in Vero E6 cells, allowing the infection of cells by non-neutralized viral particles. Then, prewarmed DMEM supplemented with 2 % fetal bovine serum (FBS) and 2 % carboxymethylcellulose (CMC) was gently added to the plates and incubated for 4–5 days at 37 °C and 5 % CO_2 to allow the viral plaque formation. Cells were fixed with 4 % formaldehyde for 2 h and stained with a 1 % solution of Naphthol blue black (Sigma) for 1 h for visualization of the plaques. The neutralizing activity was determined by plaques numbers reduction when compared to the positive control.

2.8. Cytokines measurement

Mice were euthanized thirty days after administration of the booster dose. Spleens were removed, and splenocytes were isolated by maceration in a 100 μm pore cell strainer (Cell Strainer, BD Falcon). Ammonium-chloride-potassium (ACK) buffer was used for red blood cells lysis and the cell number was adjusted to 1×10^6 cells/well. Splenocytes were stimulated with 10 μg/mL of RBD, N, or SpiN protein for 72 h at 37 °C in 5 % CO_2. The medium was used as a negative control and Concanavalin A (Sigma) at 5 μg/mL was used as a positive control. For Cytometric Bead Array (CBA) assay, beads specific for each cytokine were mixed and incubated with the supernatant culture or standard in the presence of the PE reagent for 2 h at RT protected from the light. The samples were washed with wash buffer and the samples were acquired in FACSVerse (BD Bioscience).

2.9. Determination of viral load by qRT-PCR

A fragment of the left lobe of the lung was collected in Trizol Reagent (Invitrogen) and stored at −80 °C. At the time of RNA extraction, samples were macerated using the TissueLyser LT (Qiagen), and the RNA was extracted according to the manufacturer's instructions. To quantify the viral load, a qRT-PCR reaction was performed with GoTaq Probe 1-step (Promega), primers (Fw: 5′ACAGGTACGTTAATAGTTAATAGCGT3′ and Rv: 5′ATATTGCAGCAGTACGCACACA 3′), probe (FAM-ACACTAGCCATCCTTACTGCGCTTCG-BBQ) and 75 ng RNA, according to the manufacturer's instructions. A standard curve made with serial dilutions of the plasmid containing the SARS-CoV-2 E gene was used to quantify the pulmonary viral load in challenged animals.

2.10. Flow cytometry

B and T cells were evaluated in SpiN-Tec immunized mice (splenocytes) and animals immunized and challenged with the Omicron variant (lung and splenocytes). Splenocytes from immunized mice were obtained thirty days after administration of the second dose and on 5 DPI in immunized and challenged mice. The animals were euthanized and splenocytes were isolated by spleen maceration using a 100 μm pore cell strainer (Cell Strainer, BD Falcon), followed by erythrocytes lysis with ammonium-chloride-potassium (ACK) buffer. The cell number was adjusted to 2×10^6 cells/well for intracellular staining. Splenocytes from immunized mice were stimulated with 10 μg/mL of SpiN protein for 24 h. PMA (50 ng/mL), Ionomycin (500 ng/uL), Golgi Plug (BD Bioscience), and Stop Golgi (BD Bioscience) were added in the last 6 h of culture [15]. Mice lungs were perfused with cold PBS and then digested with 100 μg/mL liberase (Roche) at 37 °C for 30 min. Cells were filtered using a 100 μm pore cell strainer (Cell Strainer, BD Falcon) and purified using a 30 % isotonic Percoll gradient. Erythrocytes were lysed with ammonium-chloride-potassium (ACK) buffer and the cell number was adjusted to 2×10^6 cells/well. Lung cells and splenocytes from challenged mice were stimulated with PMA (50 ng/mL) and Ionomycin (500 ng/uL) for 4 h added with Golgi Plug (BD Bioscience) and Stop Golgi (BD Bioscience).

Lung cells and splenocytes were stained with Live/Dead stain (Acqua, Invitrogen) for 20 min at 4 °C in the dark, incubated with FcBlock (BD Bioscience) for 20 min at 4 °C and then stained with anti-CD3 (eFluor450; Cat. # 48–0032-82; 1:100; eBioscience or PerCP-Cy5.5; Cat. # 551163; 1:100; BD Bioscience), anti-CD4 (Fitc; Cat. # 553729; 1:250; BD Bioscience), anti-CD8 (APC-Cy7; Cat. # 100714; 1:200; Biolegend) and anti-CD19 (PE; Cat. # 557399; 1:400; BD Bioscience). Cells were permeabilized with Cytofix/Cytoperm (BD Bioscience) for 20 min at 4 °C in the dark and incubated with anti-IFN-γ (PerCp-Cy5.5; Cat. # 45–7311-82; 1:80; eBioscience or APC; Cat. # 554413; 1:100; BD Bioscience) and anti-Granzyme B (eFluor450; Cat. # 48–8898-82; 1.25:100; Invitrogen) for 30 min at 4 °C. Gate strategies for the analyses of samples from immunized mice are showed in Supplementary Fig. 1 and from challenged mice in Supplementary Fig. 2. Representative density plots are presented in Supplementary Figs. 3a-b and Supplementary Figs. 4a-d. Flow cytometry acquisition was performed using a CytoFLEX (Beckman Coulter) and ~ 200,000 live cells were acquired. Data were analyzed using FlowJo v10.5.3 software.

2.11. $CD4^+/CD8^+$ T cell depletion and sera transfer

K18-hACE2 mice immunized with two doses of SpiN-Tec were treated with monoclonal antibodies to deplete T cells in vivo. Mice were treated on days −3, −2 and − 1 before the infection with i.p. injection of 0.5 mg/mouse of rat anti-mouse CD4a mAb (clone GK1.5; Cat. # BE0003–1; BioXCell) and 0.5 mg/mouse of rat anti-mouse CD8a mAb (clone 2.43; Cat. # BE0061; BioXCell) or 0.2 mg/mouse of rat anti-KLH IgG (clone LTF-2; Cat. # BP0090; BioXCell). T cell depletion was confirmed in blood samples by flow cytometry (Supplementary Fig. 4e). In the sera transfer experiment, one day before the infection, K18-hACE2 non-immunized mice received an i.p. injection with 200 μL of sera from mice immunized with SpiN-Tec. Antibodies levels in recipient mice were determined one day after sera transfer by Elisa (Supplementary Fig. 4f).

2.12. Safety test

SpiN-Tec immunized rats were monitored daily, and body weight, clinical signs, and survival were evaluated. Assessment of clinical signs included vocal fremitus, irritability, touch response, general activity, gripping strength, lacrimation and salivation, piloerection, general appearance, tail pinching, ataxia, ocular assessment, defecation/urination and respiration/heart rate. Body temperature was evaluated before (T0) and 3 h and 24 h after immunization (T3 and T24), on days D0 and D21. Hematological and biochemical parameters were also evaluated before immunization (D0), two days after the first dose and booster (D2 and D23) and at the end-point (D35). Normal reference values range for hematological and biochemical parameters were taken from the literature: hematological parameters, blood urea nitrogen (BUN) and creatinine [16], liver enzymes [17], and coagulation parameters [18]. The main group was euthanized two days after the booster dose (D23) and the recovery group 14 days after the booster dose (D35). During the necropsy, macroscopic alterations were investigated in organs like adrenal glands, spleen, brain, heart, kidneys, thymus, liver, testicles, epididymis, and ovaries. These organs were weight, relative weight was calculated in relation to body weight and organ samples were submitted to histopathological analyses. The safety tests were carried out independently at the CIEnP, and the CIEnP researchers performed animal monitoring, hematological and biochemical assays, and histopathological analyses.

2.13. Histopathology

To perform the histopathological analyses, samples were fixed in 10 % formaldehyde for 7 days, processed using the PT05 TS tissue processor (LUPETEC, UK), and embedded in histological paraffin (Histosec, Sigma). Tissues were sectioned at 4 μm thickness using the RM2125 RTS microtome (Leica) and stained with hematoxylin and eosin. Two independent pathologists carried out the histopathological analyses.

2.14. Statistical analysis

Statistical analysis was performed using the Prism 8.0 software (GraphPad Inc., USA). Data distribution was verified using the D'Agostino & Pearson test. When the sample size ('n') was sufficient to calculate the data distribution but the data did not pass the normality test, the presence of outliers was assessed using Grubb's test. The antibody titers with prime or prime/boost were compared using the Wilcoxon matched-pairs signed rank test. For comparison between non-immunized and immunized groups, the *t*-test or Mann-Whitney *U* test was performed, according to data distribution. Multiple comparisons analyses were performed using one-way ANOVA followed by the post-hoc Bonferroni test or Kruskal-Wallis followed by the post-hoc Dunn's test, according to data distribution. For survival analyses, the log-rank test was used. Significant differences were considered p values ≤ 0.05.

3. Results

3.1. SpiN-Tec is highly immunogenic and protects K18-hACE2 mice from challenge with the Wuhan isolate

Mice ($n = 4$ mice/group or more) were immunized with two doses of SpiN-Tec (10 μg or 20 μg) three weeks apart by intramuscular injection. As a control group, mice received only adjuvant (CTVad). A blood sample was collected two days before the booster dose for determination of antibody titers, and the animals were euthanized thirty days after the boost to evaluate humoral and cellular immune response (Fig. 1). Immunized mice developed high titers of specific antibodies against proteins from SARS-CoV-2 and SpiN. Different levels of antibody against RBD, N, or SpiN were observed (Fig. 2a-c). High titers of total anti-RBD IgG were observed in mice from the immunized groups. Higher levels of total anti-N and anti-SpiN IgG were observed independently of the dose (Fig. 2a). Since IgG switching is regulated by cytokines, we also investigated the titers of IgG subsets (IgG1 and IgG2c) after immunization with SpiN-Tec, to understand the cytokine responses induced by SpiN-Tec. Some animals did not produce anti-RBD IgG1 with one dose of SpiN-Tec. However, a high anti-RBD IgG1 titer was obtained after prime-boost with 20 μg of SpiN-Tec (Fig. 2b). Similar levels of IgG1 anti-N and anti-SpiN were observed regardless of the dose administered (10 μg or 20 μg) (Fig. 2b). High IgG2c anti-RBD and anti-N titers were observed after the second dose (Fig. 2c). IgG2c anti-SpiN titers were lower compared to anti-RBD and anti-N titers (Fig. 2c). Importantly, no statistically significant difference was observed in antibody levels induced by prime-boost protocol using 10 μg or 20 μg of SpiN-Tec for the IgG subclasses evaluated. Culture supernatants of splenocytes from immunized mice and restimulated in vitro with RBD, N, or SpiN protein showed increased production of IFN-γ, TNF, IL-6, IL-17, and IL-2 ($p < 0.01$) (Fig. 2d-e). In contrast, IL-4 was only detected in the supernatants of splenocytes from immunized mice restimulated with N and SpiN and IL-10 in cultures restimulated with RBD and SpiN ($p < 0.05$) (Fig. 2e). Regarding the cellular immune response, a high number of $CD8^+$ T cells producing IFN-γ was observed in splenocytes from immunized mice non-stimulated (medium) ($p < 0.05$). Higher number of $CD4^+$ and $CD8^+$ T cells producing IFN-γ in SpiN-Tec immunized mice restimulated with SpiN associated with PMA/Ionomycin were observed, the numbers being more pronounced for $CD8^+$ T cells ($p < 0.01$) (Fig. 2f). As expected, in control experiments, splenocytes that were stimulated with PMA/Ionomycin, no difference was observed between the groups (Fig. 2f). To determine its protection capacity, SpiN-Tec immunized K18-hACE2 mice (ACE-2) and K18-hACE2 deficient in B cells mice (ACE-2/B-KO) were challenged with the Wuhan isolate and followed for 12 days (Fig. 1 – red line). ACE-2 mice immunized with SpiN-Tec (dark blue lines) did not lose weight ($p < 0.05$) and showed 100 % survival ($p < 0.01$) (Fig. 2g-h). In contrast, the majority of immunized ACE-2/B-KO mice lost weight, and around 50 % recovered and survived (light blue dotted lines). As expected, all animals from control groups (CTVad + Vehicle) lost weight and died up to 10DPI (black and gray lines) (Fig. 2g-h).

3.2. SpiN-Tec protects K18-hACE2 mice against Omicron variant by cellular and humoral immune response

SpiN-Tec immunized K18-hACE2 mice challenged with the Omicron variant were euthanized at 5 DPI, and the viral load was evaluated in lung samples by qPCR. Immunization with SpiN-Tec reduced viral RNA by more than 100-fold, compared to the control group ($p < 0.01$) (Fig. 3a). Histopathological analyses of lungs from the control, non-immunized group showed a focal alveolar collapse of moderate intensity (yellow arrow), congested blood vessels (red arrow), mild hemorrhage (green arrow) associated with the presence of a mixed inflammatory infiltrate located in the perivascular region (black arrow), and fibrino-leukocytic exudate in the alveolar spaces (blue arrow)

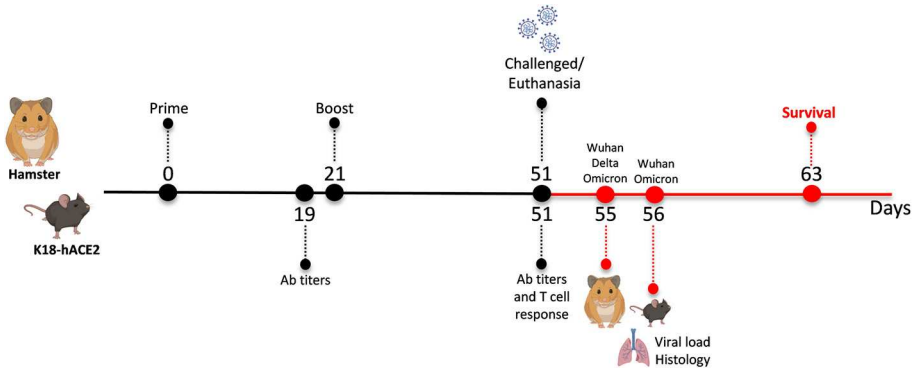

Fig. 1. Schematic representation of mice and hamsters study design. Animals were immunized via i.m. with two doses of SpiN-Tec, 21 days apart. A blood sample was collected two days before the booster dose (D19) to evaluate antibody titer. Thirty days after the boost (D51), some animals were euthanized for evaluation of the immunogenicity of SpiN-Tec, and another part was challenged with SARS-CoV-2. SpiN-Tec immunized K18-hACE2 mice were challenged with 5×10^4 PFU of Wuhan strain and were monitored daily until D63 for survival. K18-hACE2 mice immunized with SpiN-Tec and challenged with 2.5×10^4 PFU of Omicron variant were euthanized five days post-challenged (D56), and lung samples were collected to evaluate viral load and histopathology. SpiN-Tec immunized hamsters were challenged with 1×10^5 PFU for all variants and euthanized four days after being challenged (D55) to evaluate viral load and histopathology in the lungs.

(Fig. 3b). On the other hand, SpiN-Tec immunized K18-hACE2 mice showed preserved tissue architecture with inflammatory infiltrate in the perivascular region (black arrow) (Fig. 3c). We also evaluated T response during infection with the Omicron variant, since T cell epitopes were highly conserved between Wuhan and Omicron variant (Supplementary Tables 1 and 2). SpiN-Tec immunized K18-hACE2 mice showed a strong cellular response with an increased number of total T cells ($CD3^+$) ($p < 0.01$), $CD4^+$ ($p < 0.05$), and $CD8^+$ ($p < 0.05$) T cells at 5 DPI in both the lung and spleen (Fig. 3d and g). On the other hand, no statistically significant difference was observed for B cells ($CD19^+$) in both organs (Fig. 3d and g). In addition, a higher number of $CD8^+$ T cells producing IFN-γ ($p < 0.01$) (Fig. 3e) and Granzyme B ($p < 0.05$) (Fig. 3f) was detected in the mice lungs of SpiN-Tec immunized and challenged with Omicron variant. In the spleen samples, a higher number of both subsets of T cells ($CD4^+$ and $CD8^+$) producing IFN-γ were observed ($p < 0.01$) (Fig. 3g), as well as, $CD8^+$ T cells producing Granzyme B ($p < 0.01$) (Fig. 3i). To elucidate the role of T cells in the protection against the Omicron variant, SpiN-Tec immunized K18-hACE2 mice were depleted of T cells with specific monoclonal antibodies before the challenge with the Omicron variant. SpiN-Tec immunized mice treated with isotype control antibody (αKLH) showed a significant reduction of viral load in the lung in comparison to control group ($p < 0.001$). In contrast, SpiN-Tec immunized mice that were treated with antibodies against T cells (αCD4/αCD8) presented a lower reduction in lung viral load in comparison to the control group ($p < 0.05$) (Fig. 3j). However, in the nasal wash, T cells depleted immunized mice exhibited a higher viral load in comparison to non-depleted mice ($p < 0.05$), with a viral load similar to control group (Fig. 3k). Sera transfer was performed to evaluated the role of the antibodies in the protection against the Omicron variant. K18-hACE mice that received sera transfer from SpiN-Tec immunized mice showed a reduction of around 10-fold in viral load in lung samples ($p < 0.01$) (Fig. 3l). However, no difference was observed in the viral load of the nasal wash (Fig. 3m).

3.3. Homologous and heterologous prime/boost protocols using SpiN-Tec induce antibodies against the Omicron variant

Mice were immunized with ChAdOx1 and SpiN-Tec in homologous and heterologous prime/boost schedules (Fig. 4a). Mice that received 2 doses of SpiN-Tec (10 μg) developed high titers of total IgG, IgG1, and IgG2c against RBD from the Omicron variant (Figs. 4b-d). In contrast, mice that received either one or 2 doses of ChAdOx1 (1×10^{10} PV) have similar titers of total IgG, IgG1, and IgG2c against RBD from the Omicron variant (Figs. 4b-d). The heterologous prime/boost protocol (ChadOx1/SpiN-Tec) induced higher levels of total IgG ($p < 0.05$) (Fig. 4b). Although immunization with SpiN-Tec does not result in the production of neutralizing antibodies, higher levels of nAbs against Wuhan isolate were detected when SpiN-Tec was used as a booster dose (green circles), compared to a single dose of ChAdOx1 ($p < 0.0001$) or two doses of ChAdOx1 ($p = 0.001$) (Fig. 4e). The ChAdOx1 homologous prime/boost (filled red circles) did not enhance nAb titers compared to a single dose of ChAdOx1 (empty red circles) (Fig. 4e). We also evaluated the nAb anti-Omicron titers. Although not statistically significant, the boost with SpiN-Tec induced a slight increase in the median of nAb titers against Omicron variant (Fig. 4f). The T cell response was also evaluated using homologous and heterologous prime/boost immunization protocols. Higher production of IFN-γ by splenocytes was observed for both heterologous (ChAdOx1/SpiN-Tec) and homologous (ChAdOx1/ChAdOx1) immunization protocol, in response to restimulation with RBD ($p < 0.001$) and SpiN ($p < 0.5$) recombinant proteins in comparison to control group (Fig. 4g). No statistically significant difference was observed between heterologous (ChAdOx1/SpiN-Tec) and homologous (ChAdOx1/ChAdOx1) immunization protocols (Fig. 4g).

3.4. SpiN-Tec induces humoral immune response in hamsters

We have also immunized hamsters with two doses of SpiN-Tec three weeks apart by intramuscular injection and antibody titers were evaluated two days before and thirty days after the boost (Fig. 1). As observed in the mice model, hamsters immunized with SpiN-Tec also showed different levels of antibody against RBD, N, or SpiN. Total anti-RBD IgG titer after the prime-boost was similar independently of the dose used (25 μg or 50 μg) (Fig. 5a). Total anti-N and anti-SpiN IgG titers were more homogeneous within groups (Fig. 5a). Anti-RBD IgG1 was not detected (Fig. 5b). High IgG1 titers after two doses of SpiN-Tec were detected for N and SpiN (Fig. 5b). Importantly, only anti-SpiN IgG1 titer showed a significant difference between the 2 doses tested (25 μg or 50 μg), being more pronounced for SpiN-Tec 50 μg (Fig. 5b). Anti-RBD IgG2/IgG3 production was observed in all animals after prime-boost (Fig. 5c). There was no increase in anti-N and anti-SpiN IgG2/IgG3 after the booster dose for the tested doses (25 μg or 50 μg) (Fig. 5c).

3.5. SpiN-Tec protects hamsters from challenge with Wuhan isolate, Delta and Omicron variants

Hamsters are considered a model for moderate COVID-19 since they control the infection and recover [19,20]. Immunized animals were challenged with the Wuhan isolate, Delta and Omicron variants and euthanized 4 days after infection to measure viral load and to evaluate histopathology findings. Hamsters immunized with SpiN-Tec and

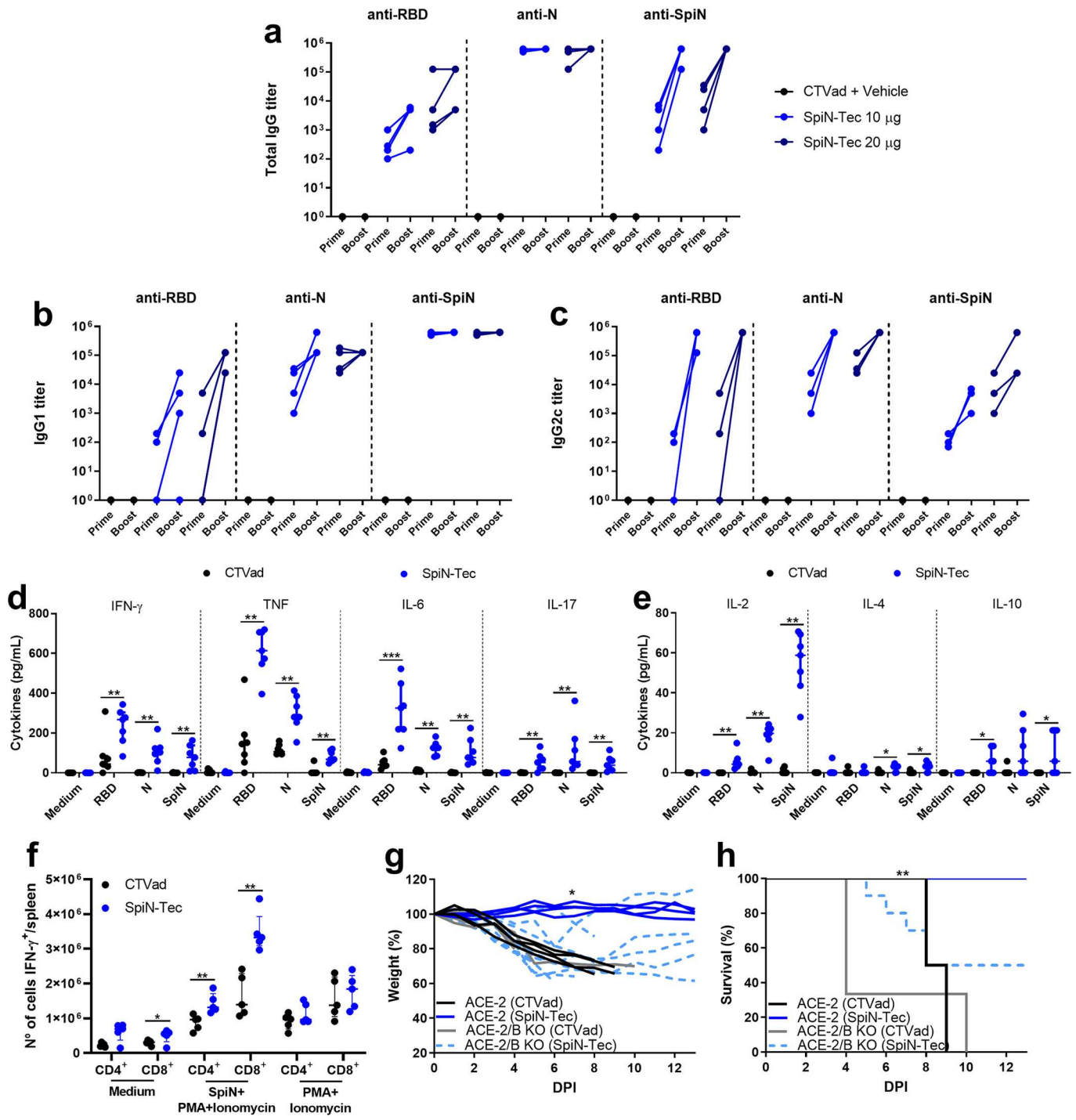

Fig. 2. SpiN-Tec immunogenicity and protection against Wuhan isolate in mice model. (a) Total anti-RBD, anti-N, and anti-SpiN IgG titers in mice that received CTVad + Vehicle (black circles), SpiN-Tec 10 μg (light blue circles) or SpiN-Tec 20 μg (dark blue circles) after first immunization (prime) or two doses (prime/boost) [$n = 4$ mice/group]. **(b)** Anti-RBD, anti-N, and anti-SpiN IgG1 titers in mice that received CTVad + Vehicle (black circles), SpiN-Tec 10 μg (light blue circles) or SpiN-Tec 20 μg (dark blue circles) after first immunization (prime) or two doses (prime/boost) [n = 4 mice/group]. **(c)** Anti-RBD, anti-N, and anti-SpiN IgG2c titers in mice that received CTVad + Vehicle (black circles), SpiN-Tec 10 μg (light blue circles) or SpiN-Tec 20 μg (dark blue circles) after first immunization (prime) or two doses (prime/boost) [n = 4 mice/group]. IFN-γ, TNF, IL-6, IL-17 **(d)** and IL-2, IL-4, and IL-10 **(e)** produced by splenocytes from CTVad + Vehicle (black circles) or SpiN-Tec 10 μg (blue circles) mice after 72 h of incubation with medium (negative control) and restimulation with recombinant RBD, N or SpiN protein [$n = 7$ mice/group]. **(f)** Number of $CD4^+$ and $CD8^+$ T cells producing IFN-γ from splenocytes of mice that received CTVad + Vehicle (black circles) or were immunized with SpiN-Tec 10 μg (blue circles), after restimulation in vitro with SpiN protein for 24 h [n = 7mice/group]. Body weight **(g)** and survival **(h)** of K18-hACE2 mice that received CTVad + Vehicle (black lines) or SpiN-Tec 10 μg (blue lines) and K18-hACE2/B-KO that received CTVad + Vehicle (gray lines) or SpiN-Tec 10 μg (light blue dotted lines) and were challenged with the Wuhan isolate of SARS-CoV-2 [K18-hACE2: n = 4 mice/group; K18-hACE2/B-KO: 6–10 mice/group] [* K18-hACE2: CTVad + Vehicle vs SpiN-Tec]. The statistical analysis of cytokines production and IFN-γ producing T cells was carried out using Mann-Whitney *U* test, lines represent median with an interquartile range. The statistical analysis of body weight curves was performed by area under the curve followed by the Kruskal-Wallis test followed by the post-hoc Dunn's test. The statistical analysis of survival was performed using the log-rank test. *$p < 0.05$; **$p < 0.01$; ***$p < 0.001$. (For interpretation of the references to colour in this figure legend, the reader is referred to the web version of this article.)

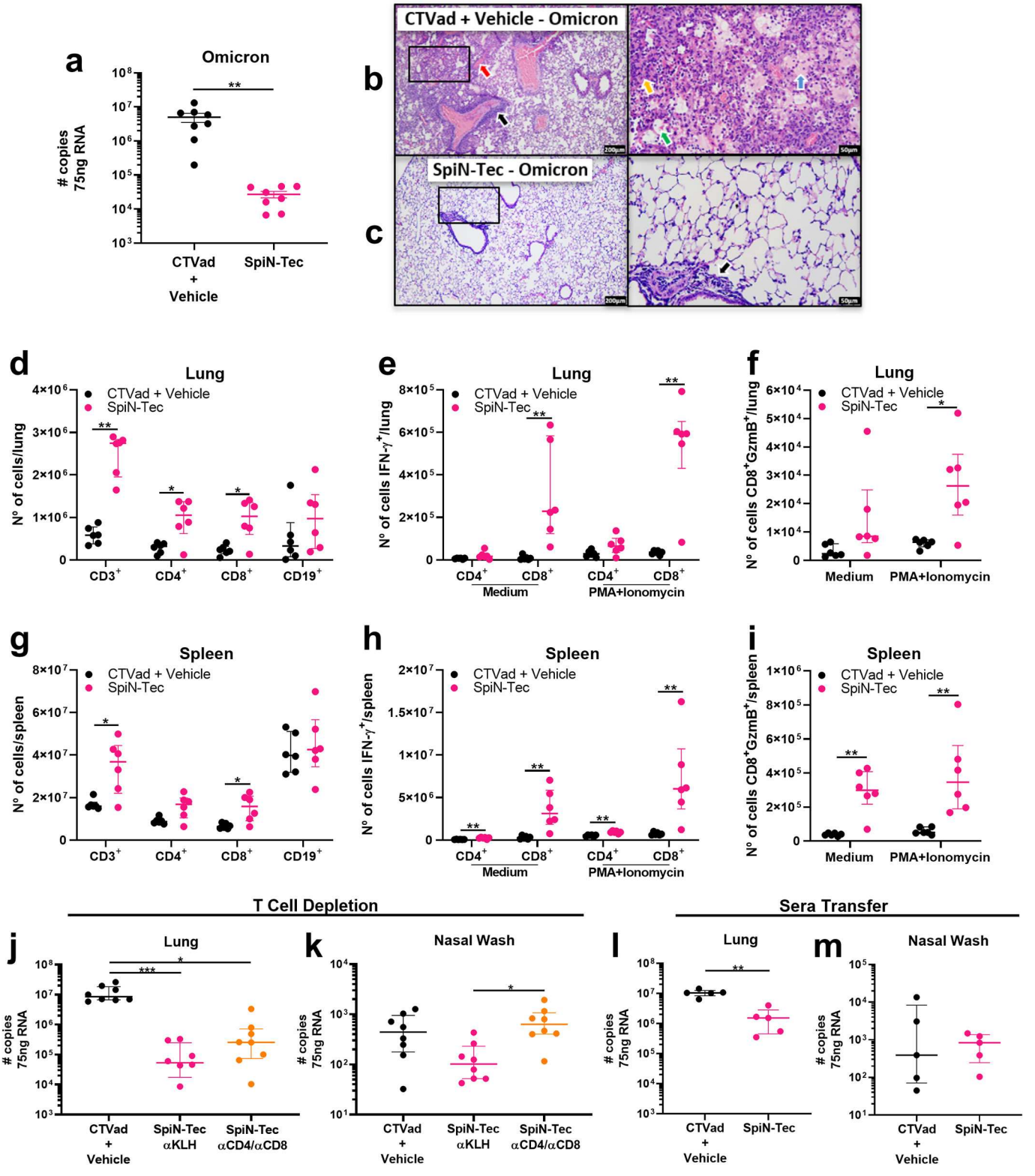

(caption on next page)

Fig. 3. SpiN-Tec protection against the Omicron variant in mice model. (a) Lung viral load from CTVad + Vehicle (black circles), or SpiN-Tec 10 μg immunized K18-hACE2 mice (pink circles) and challenged with the Omicron variant at 5 DPI [$n = 8$ mice/group]. Histopathological sections of lungs from CTVad + Vehicle **(b),** and SpiN-Tec 10 μg immunized K18-hACE2 mice **(c)** at 5 DPI [n = 8 mice/group]. The inflammatory infiltrate in the perivascular region (black arrow), vascular congestion (red arrow), alveolar collapse (yellow arrow), hemorrhage (green arrow), and edema (blue arrow) at 10× (200 μm) and 40× (50 μm) magnification. **(d)** Number of total T cells ($CD3^+$) and subsets ($CD4^+$ and $CD8^+$) and B cells ($CD19^+$) in the lungs of K18-hACE2 mice that received CTVad + Vehicle (black circles) or SpiN-Tec (pink circles) at 5 DPI with Omicron variant [$n = 6$ mice/group). Number of $CD4^+$ and $CD8^+$ T cells producing IFN-γ **(e)** or $CD8^+$ T cells producing Granzyme B **(f)** in the lungs of K18-hACE2 mice that received CTVad + Vehicle (black circles) or SpiN-Tec (pink circles) at 5 DPI with Omicron variant [n = 6 mice/group]. **(g)** Number of total T cells ($CD3^+$) and subsets ($CD4^+$ and $CD8^+$) and B cells ($CD19^+$) in the spleen of K18-hACE2 mice that received CTVad + Vehicle (black circles) or SpiN-Tec (pink circles) at 5 DPI with Omicron variant [n = 6 mice/group]. Number of $CD4^+$ and $CD8^+$ T cells producing IFN-γ **(h)** or $CD8^+$ T cells producing Granzyme B **(i)** in the spleen of K18-hACE2 mice that received CTVad + Vehicle (black circles) or SpiN-Tec (pink circles) at 5 DPI with Omicron variant [n = 6 mice/group]. Viral load in lung **(j)** and nasal wash **(k)** of K18-hACE2 mice immunized with SpiN-Tec treated with isotype control antibodies (pink circles) or anti-T cells antibodies (orange circles) at 5 DPI with Omicron variant [n = 8 mice/group]. Viral load in the lung **(l)** and nasal wash **(m)** of K18-hACE2 mice that received sera transfer from mice that received CTVad + Vehicle (black circles) or SpiN-Tec immunized (pink circles) at 5 DPI with Omicron variant [$n = 5$ mice/group]. The statistical analysis of viral load in mice challenged with Omicron was performed using the unpaired *t*-test. The statistical analysis of T and B cells, T cells producing IFN-γ, and Granzyme B were performed using the Mann-Whitney U test, lines represent the median with the interquartile range. The statistical analysis of T cell depletion was performed by the Kruskal-Wallis test followed by post-hoc Dunn's test. The statistical analysis of the viral load of mice that received sera transfer was performed using the Mann-Whitney U test. $*p < 0.05$; $**p < 0.01$; $***p < 0.001$. (For interpretation of the references to colour in this figure legend, the reader is referred to the web version of this article.)

challenged with the Wuhan isolate showed a significant reduction (65 %) in viral RNA in lung samples in comparison to control group ($p < 0.01$) (Fig. 6a). Non-immunized hamsters challenged with the Wuhan isolate developed diffuse interstitial pneumonia, with the presence of congestion (red arrow), associated with a focal mononuclear inflammatory infiltrate characterized by neutrophilic predominance in the alveolar septum (black arrow) (Fig. 6b). In contrast, hamsters immunized with SpiN-Tec and challenged with the Wuhan isolate showed preserved lung tissue architecture without morphological alterations (Fig. 6c). Immunized hamsters challenged with the Delta variant also showed a significant reduction (65 %) on viral RNA load in the lungs in comparison to the non-immunized group ($p < 0.01$) (Fig. 6d). Regarding histopathological evaluation, hamsters from the control group (CTVad + Vehicle) challenged with the Delta variant showed pulmonary involvement, with focal septal thickening (brace), hemorrhagic focus (green arrow), and congestion (red arrow) associated with peribronchovascular mononuclear inflammatory infiltrate (black arrow) (Fig. 6e). In contrast, the group immunized with SpiN-Tec showed preserved lung architecture and airspace, with the presence of congestion (red arrow) (Fig. 6f). SpiN-Tec immunized hamsters challenged with the Omicron variant exhibited around 10-fold reduction (~87 %) in viral RNA in lung samples in comparison to the control group ($p < 0.01$) (Fig. 6g). Non-immunized hamsters challenged with the Omicron variant presented an inflammatory infiltrate with the predominance of mononuclear cells, concentrated in the peribronchovascular region (black arrow), associated with edema (blue arrow) and septal thickening (brace) demonstrating moderate involvement of the lung (Fig. 6h). On the other hand, SpiN-Tec immunized animals and challenged with the Omicron variant presented mild lung involvement, with preserved lung tissue architecture associated with a focal hemorrhage (green arrow) and septal thickening (brace) (Fig. 6i).

3.6. SpiN-Tec is immunogenic and is safe for rats

To evaluate SpiN-Tec toxicity and safety, Sprague Dawley rats were immunized with two doses of SpiN-Tec three weeks apart by intramuscular injection. Blood samples were collected before immunization (D0), two days after the first and second dose (D2 and D23, respectively), and at endpoint (D35) for evaluation of hematological and biochemical parameters. Humoral response was assessed 14 days after the first dose and at the endpoint (D14 and D35, respectively). Some animals were euthanized two days after the second dose (D23 - Main Group) and another group was euthanized at the endpoint (D35 – Recovery Group) (Fig. 7a). Rats immunized with two doses of SpiN-Tec developed high titers of specific antibodies against proteins from SARS-CoV-2 and SpiN. Different antibody levels were observed against RBD, N, and SpiN, with higher total IgG titers of anti-N and anti-SpiN, compared to anti-RBD for both females and males (Fig. 7b). Similar results were observed for IgG1 titers, with higher anti-N and anti-SpiN levels for both females and males (Fig. 7c). Although most of the animals did not produce anti-RBD IgG2b with one dose of SpiN-Tec, all animals produced significant titers after the SpiN-Tec booster dose (Fig. 7d). Higher IgG2b titers anti-N and anti-SpiN were detected after two doses of SpiN-Tec (Figs. 7d).

Body weight was evaluated daily for all animals from the main groups (Fig. 8a). There was no statistically significant difference among groups. All animals gained weight over time, being more pronounced in male rats, regardless the experimental group (Fig. 8a). Similar result was observed for rats from the recovery group (Supplementary Fig. 5a). The body temperature was evaluated before immunization (T0), 3 h, and 24 h after the first (D0) and booster dose (D21) (Fig. 8b). As expected, some alterations in body temperature were detected. However, it is important to highlight that the body temperature remained within the normal reference value range (35.9–37.5 °C) for all experimental groups from the main group (Fig. 8b). A similar result was observed to the animals from recovery group (Supplementary Fig. 5b). Regarding hematological parameters, an increase in the white blood cell count (WBC) (Supplementary Fig. 5c - upper panels) was observed for both females and males after immunizations. However, the WBC count remained within the normal reference value range (3–17 × 10^3 cells/μL). In addition, at the endpoint (D35) the WBC values returned to initial levels (D0 - baseline). Similarly, alterations in the percentage of lymphocytes, monocytes, and neutrophils remained within the normal reference value range (Supplementary Fig. 5c). Variations in the number of red blood cells (RBC) and hemoglobin were also observed, but all were within the normal reference value range (Supplementary Fig. 5c).

The liver and kidney functions were evaluated by measuring liver enzymes, blood urea nitrogen (BUN), and creatinine (Fig. 8c). The alanine aminotransferase (ALT) and aspartate aminotransferase (AST) liver enzymes did not show alterations during the experimental time for both females and males of all experimental groups (Fig. 8c – upper panels). The BUN and creatinine values were also within the normal range (Fig. 8c – lower panels). We also investigated alterations in coagulation parameters (Fig. 8d). An increase in fibrinogen levels were observed in animals that received adjuvant alone or SpiN-Tec (Fig. 8d – upper panels). However, the fibrinogen levels returned to basal levels (D0) at D35 (recovery group). Some alterations were detected for prothrombin time and activated partial thromboplastin time (aPTT), and the levels did not return to basal levels in some experimental groups (Fig. 8d – middle panels). It is important to observe that the control group (vehicle) also presented alterations in prothrombin and aPTT time. The platelets count showed some variation among time, but all within the normal reference value range (Fig. 8d – lower panels).

No significant alteration in clinical signs was observed during the safety and toxicity test, and all animals survived. No alteration was

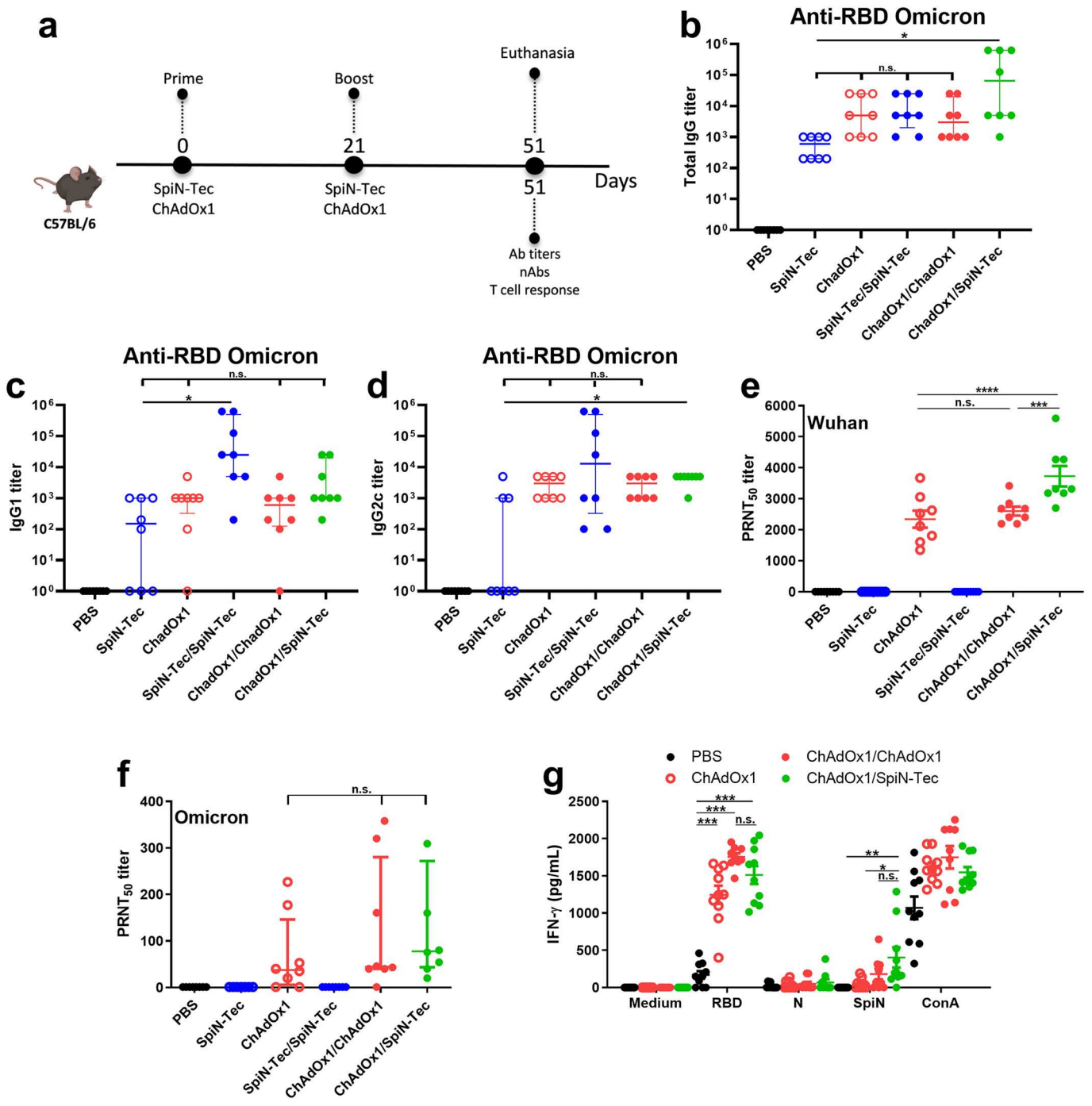

Fig. 4. Immunogenicity of homologous and heterologous prime/boost vaccination with SpiN-Tec. (a) Animals were immunized via i.m. with one dose of SpiN-Tec or ChadOx1, two doses of SpiN-Tec or ChadOx1 (homologous protocol), or one dose of ChadOx1 followed by one dose of SpiN-Tec (heterologous protocol), 21 days apart. Thirty days after the boost (D51), the animals were euthanized for evaluation of the immunogenicity. Anti-RBD Omicron total IgG **(b)**, IgG1 **(c)**, and IgG2c **(d)** titers in mice that received PBS (black circles), SpiN-Tec (empty blue circle), ChAdOx1 (empty red circles), SpiN-Tec/SpiN-Tec (filled blue circles), ChAdOx1/ChAdOx1 (filled red circles) or ChAdOx1/SpiN-Tec (filled green circles) [n = 8 mice/group]. nAbs titers against Wuhan isolate **(e)** or Omicron variant **(f)** in mice that received PBS (black circles), SpiN-Tec (empty blue circle), ChAdOx1 (empty red circles), SpiN-Tec/SpiN-Tec (filled blue circles), ChAdOx1/ChAdOx1 (filled red circles) or ChAdOx1/SpiN-Tec (filled green circles) [n = 8 mice/group]. **(g)** IFN-γ produced by splenocytes from mice that received PBS (black circles), SpiN-Tec (empty blue circle), ChAdOx1 (empty red circles), SpiN-Tec/SpiN-Tec (filled blue circles), ChAdOx1/ChAdOx1 (filled red circles) or ChAdOx1/SpiN-Tec (filled green circles) [$n = 10$ mice/group]. The statistical analysis of IgG titer was performed using the Kruskal-Wallis test followed by the post-hoc Dunn's test. The statistical analysis of nAbs was performed using One-Way ANOVA followed by post-hoc Bonferroni test (Wuhan) or Kruskal-Wallis followed by post-hoc Dunn's test (Omicron). The statistical analysis of IFN-γ production was performed using One-Way ANOVA followed by post-hoc Sidak's test. One outlier was removed in the following groups: PBS (N and SpiN), ChAdOx1 (N and SpiN), and ChAdOx1/SpiN-Tec (N). $^{*}p < 0.05$; $^{**}p < 0.01$; $^{***}p < 0.001$. (For interpretation of the references to colour in this figure legend, the reader is referred to the web version of this article.)

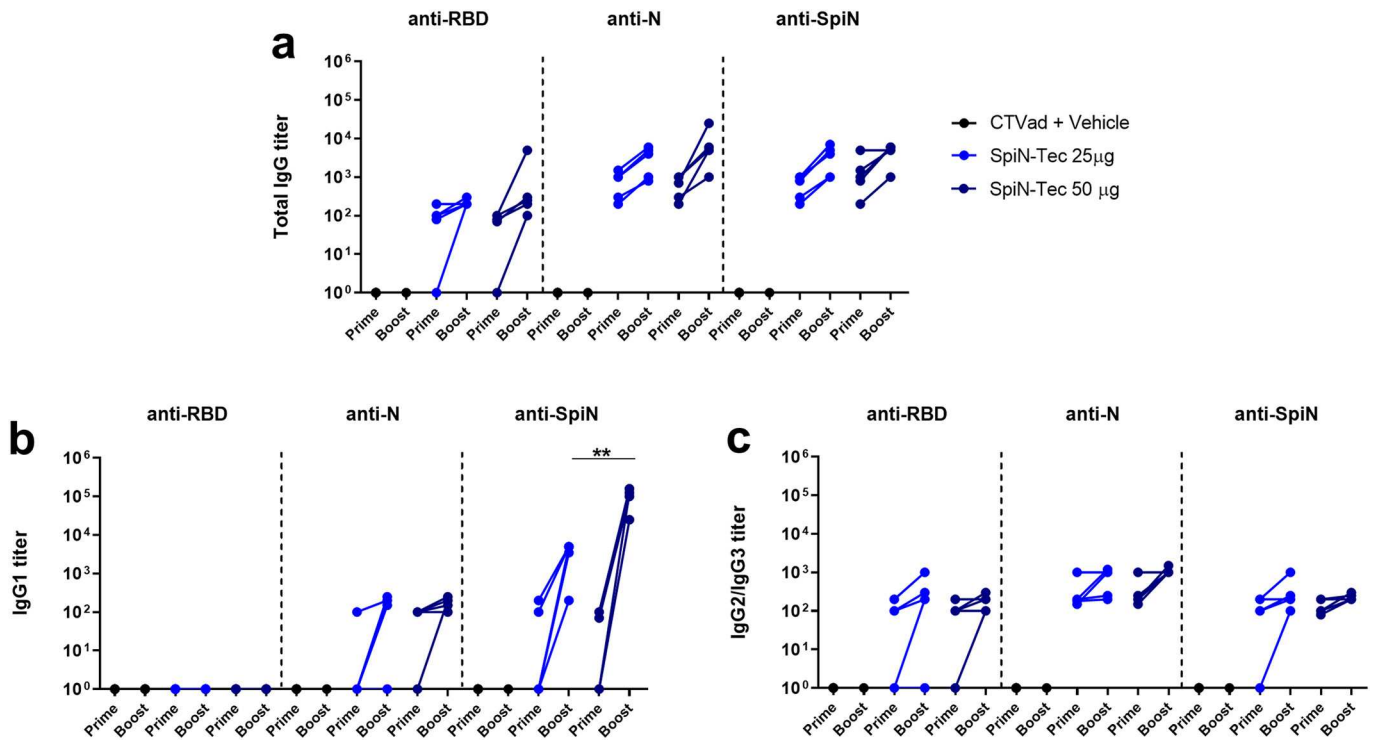

Fig. 5. SpiN-Tec immunogenicity in hamster model. (a) Total anti-RBD, anti-N, and anti-SpiN IgG titer in hamsters that received CTVad + Vehicle (black circles), SpiN-Tec 25 μg (light blue circles) or SpiN-Tec 50 μg (dark blue circles) after first immunization (prime) or two doses (prime/boost) [n = 5 animals/group]. **(b)** Anti-RBD, anti-N, and anti-SpiN IgG1 titer in hamsters that received CTVad + Vehicle (black circles), SpiN-Tec 25 μg (light blue circles) or SpiN-Tec 50 μg (dark blue circles) after first immunization (prime) or two doses (prime/boost) [n = 5 animals/group]. **(c)** Anti-RBD, anti-N, and anti-SpiN IgG2/IgG3 titer in hamsters that received CTVad + Vehicle (black circles), SpiN-Tec 25 μg (light blue circles) or SpiN-Tec 50 μg (dark blue circles) after first immunization (prime) or two doses (prime/boost) [n = 5 animals/group]. The statistical analysis of IgG titer between SpiN-Tec 25 μg and SpiN-Tec 50 μg was performed using the Mann-Whitney U test. $^{**}p < 0.01$. (For interpretation of the references to colour in this figure legend, the reader is referred to the web version of this article.)

observed at the vaccination site, such as irritation, erythema, or any other parameter evaluated in the Draize test. During the necropsy the adrenal gland, brain, heart, kidney, liver, spleen, thymus, ovary, epididymis, and testicle were removed and weighed. In the main group (D23), it was observed an increase in spleen relative weight for females and males in comparison to the control group (vehicle). However, this difference was not observed in the recovery group, euthanized at D35 (Supplementary Table 3). Furthermore, an increase in the relative weight of female kidneys was observed in the rats of the main group (D23), being normalized in the recovery group (D35) (Supplementary Table 3). No significant macroscopic findings were found in the organs evaluated during the necropsy for both the main and recovery groups. The histopathological analysis of the main group indicated edema associated with focal and diffuse inflammatory infiltrate in the site of immunization (muscle tissue). However, it is important to emphasize that the main group was euthanized 2 days after the booster dose. Regarding the recovery group, low-grade fibrosis was observed at the injection site, but without any active inflammatory reaction. In conclusion, immunization with SpiN-Tec did not show significant changes in parameters indicative of toxicity, such as mortality and/or morbidity and relevant clinical signs, indicating that the vaccine is safe.

4. Discussion

Vaccination has proved to be critically important for the control of the COVID-19 pandemic and to prevent severe disease and deaths. However, according to the update made by WHO, from April 28 to May 26, 2024, approximately 129,000 cases and 1792 fatalities were still reported worldwide. These numbers may not reflect the actual number as many countries have interrupted or changed the reporting frequency [21]. These data suggest that COVID-19 has become endemic. The monovalent COVID-19 vaccines currently in use primarily target the Spike protein or RDB (receptor-binding domain) and are capable of inducing robust humoral and cellular responses [22]. However, waning immunity over time and the emergence of VOCs, with numerous mutations in the Spike protein, have reduced the effectiveness of these vaccines, enabling breakthrough infections. Therefore, the emergence of new SARS-CoV-2 variants capable of escaping neutralizing Abs induced by vaccines based on the Spike protein from the ancestral isolate, in addition to waning immunity, has encouraged the development of new vaccines aiming to improve T-cell mediated immunity to circulating variants [23].

Importantly, different studies have shown that individuals immunized with vaccines designed with the sequence of wild-type strain Spike protein retain T cell immunity to the SARS-CoV-2 Omicron variant, and protect against severe disease caused by VOCs, even in the absence or low titers of nAbs that recognize the VOCs [3,6–8,24,25]. Thus, it is possible that the immune mediated resistance to Omicron variant is dependent on effector T cells. These findings reinforce the necessity for the development of vaccines that focus not only on nAbs, but also on T cells to control the infection. Therefore, we developed a chimeric protein composed of the full-length N-protein and the RBD portion of the Spike protein, since both proteins have been shown immunogenic and highly enriched for $CD4^+$ T and $CD8^+$ T cell epitopes [2,26–28].

In addition, to be conserved among the SARS-CoV-2 VOCs, the N is highly expressed in the host cells cytosol and is likely to be presented by the MHC class I, being a good target for cytotoxic $CD8^+$ T cells [29]. Indeed, studies performed in our laboratory and elsewhere indicate that the N protein is highly immunogenic, inducing both humoral and cellular immune responses [30–32] that control viral load in mice and hamsters challenged with SARS-CoV-2 VOCs [2,26,33,34].

Although the N protein is highly immunogenic, the RDB portion in

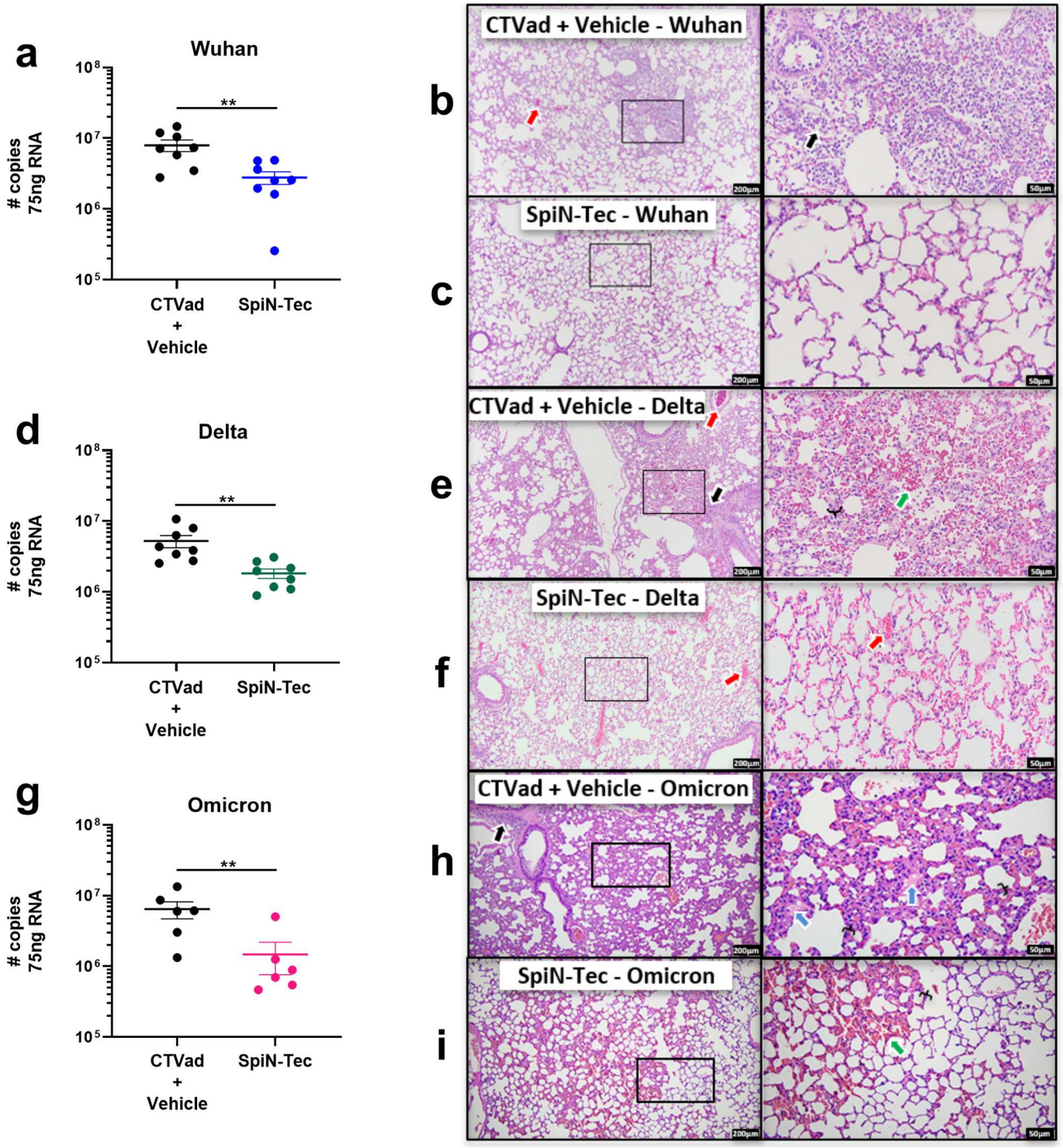

Fig. 6. Protection against variants of concern in SpiN-Tec immunized Syrian hamsters. (a) Lung viral load in CTVad + Vehicle (black circles) or SpiN-Tec 50 µg (blue circles) immunized Syrian hamsters and challenged with the Wuhan isolate at 4 DPI [n = 8 animals/group]. Histopathological sections of lungs from CTVad + Vehicle **(b)** and SpiN-Tec 50 µg **(c)** immunized hamsters and challenged with the Wuhan isolate at 4 DPI [n = 8 animals/group]. Inflammatory infiltrate in the perivascular region (black arrow), vascular congestion (red arrow). **(d)** Viral load in CTVad + Vehicle (black circles) or SpiN-Tec 50 µg (green circles) immunized hamsters and challenged with the Delta variant at 4 DPI [n = 8 animals/group]. Histopathological sections of lungs from CTVad + Vehicle **(e)** and SpiN-Tec 50 µg **(f)** immunized hamsters and challenged with Delta variant at 4 DPI [n = 8 animals/group]. Inflammatory infiltrate in the perivascular region (black arrow), vascular congestion (red arrow), hemorrhage (green arrow), and septal thickening (brace). **(g)** Viral load in CTVad + Vehicle (black circles) or SpiN-Tec 50 µg (pink circles) immunized hamsters and challenged with the Omicron variant at 4 DPI [n = 6 animals/group]. Histopathological sections of lungs from CTVad + Vehicle **(h)** and SpiN-Tec 50 µg **(i)** immunized hamsters and challenged with the Omicron variant at 4 DPI [n = 6 animals/group]. Inflammatory infiltrate in the perivascular region (black arrow), edema (blue arrow), hemorrhage (green arrow), and septal thickening (brace). Histology images represent 10× (200 µm) and 40× (50 µm) magnification. The statistical analysis of viral load was performed using an unpaired t-test (Wuhan and Delta) and Mann-Whitney U test (Omicron). $^{**}p < 0.01$. (For interpretation of the references to colour in this figure legend, the reader is referred to the web version of this article.)

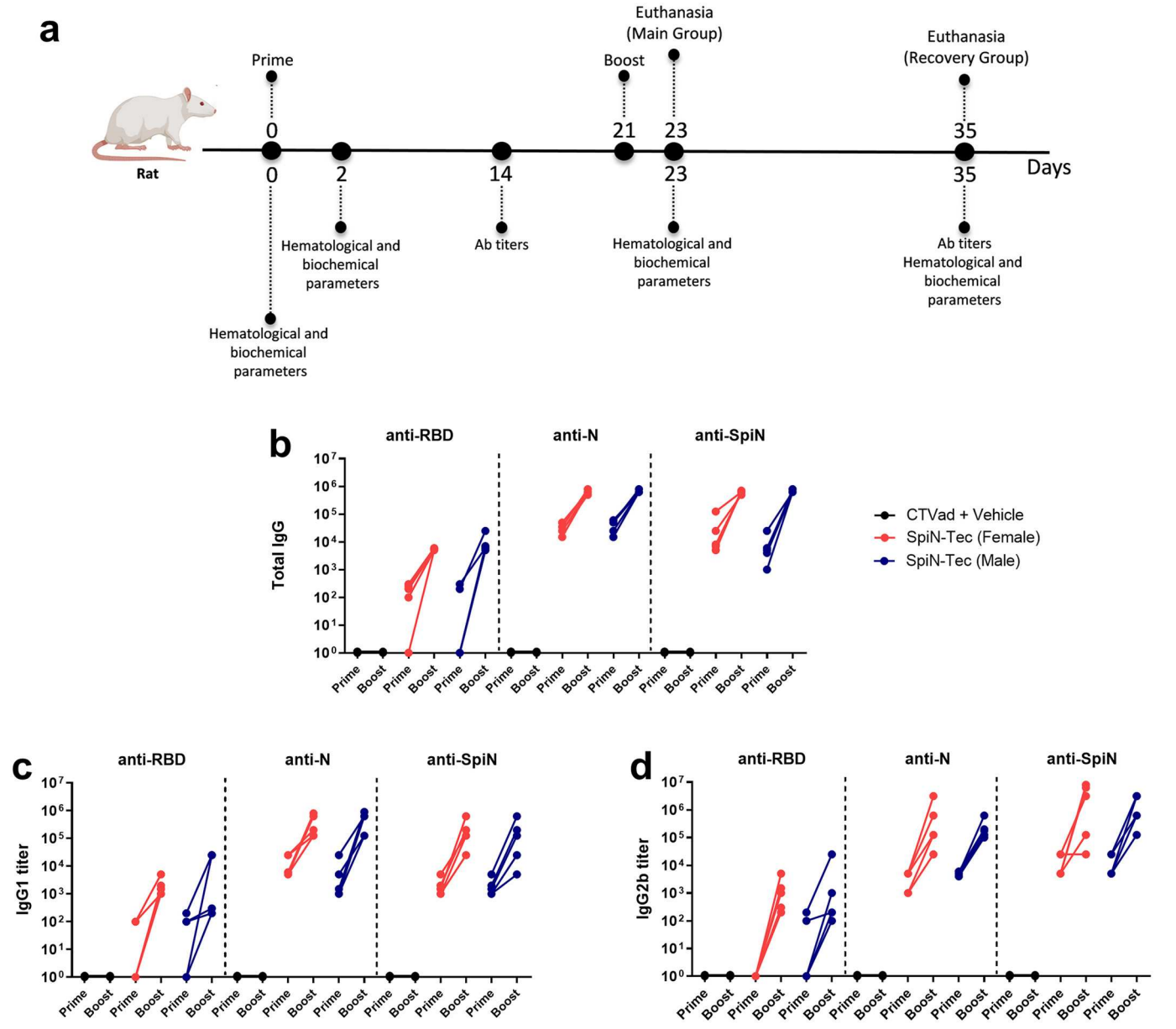

Fig. 7. SpiN-Tec immunogenicity in rat model. (a) Animals were immunized via i.m. with two doses of SpiN-Tec, 21 days apart. Blood samples were collected before immunization (D0), 2 and 14 days after the first dose (D2 and D14, respectively), two days after the booster dose (D23), and at end-point (D35). Hematological and biochemical parameters were evaluated at D0, D2, D23, and D35. Antibody titers were measured at D14 and D35. The main group was euthanized two days after the booster dose (D23) for toxicity evaluation, and the recovery group was euthanized at the end-point (D35) for safety evaluation. **(b)** Total anti-RBD, anti-N, and anti-SpiN IgG titer in female and male rats that received CTVad + Vehicle (black circles) or SpiN-Tec 100 μg (red circles – females; blue circles - males) after first immunization (prime) or two doses (prime/boost) [n = 5 rats/group]. **(c)** Anti-RBD, anti-N, and anti-SpiN IgG1 titer in female and male rats that received CTVad + Vehicle (black circles) or SpiN-Tec 100 μg (red circles – females; blue circles - males) after first immunization (prime) or two doses (prime/boost) [n = 5 rats/group]. **(d)** Anti-RBD, anti-N, and anti-SpiN IgG2b titer in female and male rats that received CTVad + Vehicle (black circles) or SpiN-Tec 100 μg (red circles – females; blue circles - males) after first immunization (prime) or two doses (prime/boost) [n = 5 rats/group]. (For interpretation of the references to colour in this figure legend, the reader is referred to the web version of this article.)

the SpiN chimeric vaccine was shown essential to protect 100 % of the mice challenged with the wild type (Wuhan) as well as the Delta and Omicron variants of SARS-CoV-2 [2]. We hypothesize that, upon infection, priming with RBD epitopes could favor helper $CD4^+$ T cells to accelerate the production of antibodies that recognize conserved regions of RBD. Importantly, despite of low levels of nAbs, a recent study demonstrates that an RBD-specific antibody triggers Fc-dependent effector functions that protect mice challenged with Omicron subvariants [35]. Like our previous report [2], studies performed elsewhere showed that an mRNA vaccine that expresses only the N protein of SARS-CoV-2, although immunogenic, modestly controlled infection by Delta and Omicron variants. Yet, in combination with an mRNA vaccine expressing the S protein, it was able to induce robust control against these variants in the lungs, with a significant reduction in the viral load in the upper respiratory tract [36].

We have previously reported the immunogenicity and efficacy of a recombinant chimeric RDB/N (SpiN) chimeric vaccine adjuvanted with Poly ICLC in mice and hamsters [2]. Aiming to approve a phase I/II clinical trial, we further investigated the immune response induced by immunization of mice and hamsters with SpiN protein adjuvanted with CTVad1 (MF59-based adjuvant). MF59 is a squalene oil-in-water emulsion with demonstrated safety and efficacy for human use and

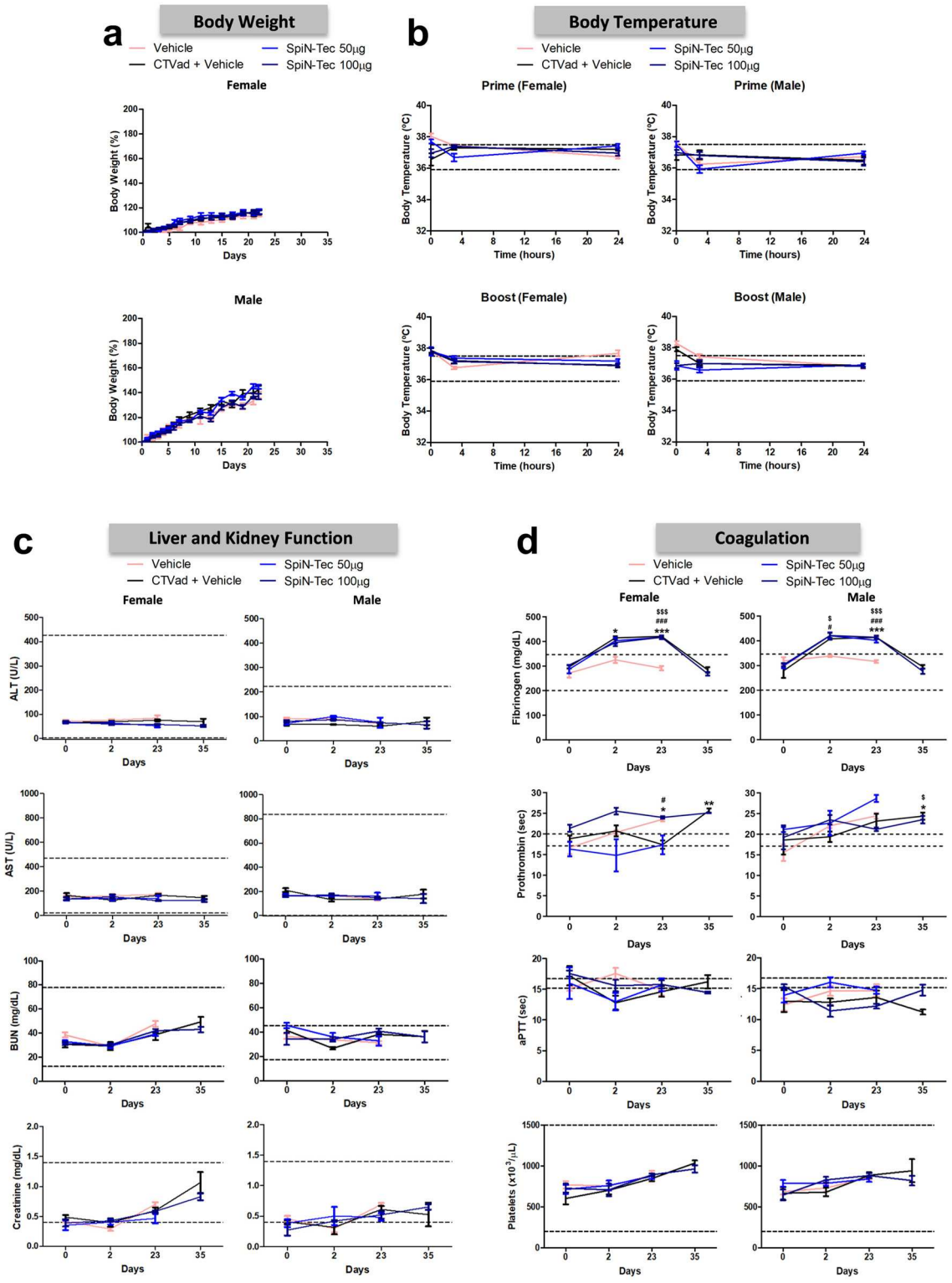

Fig. 8. Safety test in the rat model. Body weight **(a)** and temperature **(b)** of animals from the main group. **(c)** Liver and kidney functions were evaluated by measuring ALT (alanine aminotransferase), AST (aspartate aminotransferase), BUN (blood urea nitrogen), and creatinine in blood samples from animals of the main and recovery groups at different time points. **(d)** The coagulation was evaluated by measuring fibrinogen, prothrombin time, aPTT (activated partial thromboplastin time), and platelets count in blood samples from animals of the main and recovery groups at different time points. Vehicle (pink lines), CTVad + Vehicle (black lines), SpiN-Tec 50 µg (light blue lines), and SpiN-Tec 100 µg (dark blue lines). The dotted lines represent the normal reference value range for all biochemicals and hematological parameters. Some normal reference value range varies according to the sex of the animal. The statistical analysis of weight curves and body temperature was performed by area under the curve followed and one-way ANOVA followed by the post-hoc Bonferroni test. The statistical analysis of biochemical parameters was performed by one-way ANOVA followed by the post-hoc Bonferroni test. $^{*}p < 0.05$; $^{**}p < 0.01$; $^{***}p < 0.001$ (* V x CT; # V x SpiN 50 µg; $ V x SpiN 100 µg). (For interpretation of the references to colour in this figure legend, the reader is referred to the web version of this article.)

included in registered and commercially approved human vaccines [37] that enhance both humoral and cellular response [38]. Hence, we generated the SpiN-Tec vaccine containing the SpiN chimeric protein adjuvanted with CTVad1 [13].

Like SpiN associated with Poly ICLC, SpiN-Tec induced a strong humoral and cellular immune response. We observed high levels of IgG antibodies against RDB, N, and SpiN proteins and significantly increased production of IFN-γ, IL-2, and TNF, but no IL-4 produced by T cells. In addition, the IgG2 levels of anti-RBD and anti-N were higher than IgG1 in all experimental models, indicating that the SpiN-Tec vaccine induced a type I immune response.

Antibodies play a crucial role in protecting against viral infection by mechanisms such as viral neutralization, complement-dependent cytotoxicity, antibody-dependent cellular cytotoxicity (ADCC), and antibody-dependent cellular phagocytosis (ADCP), depending on the effector cell to which they bind. Cells such as Natural Killer and neutrophils express the FcγRIII receptor that could mediate ADCC. Virus-specific antibodies can exert antiviral activity by Fc-dependent antibody effector functions in SARS-CoV-2 infection [39]. Understanding of the effector functions of non-neutralizing antibodies is still limited, but non-neutralizing Abs could contribute to immunity to SARS-CoV-2 through their effector functions acting synergistically [40]. Non-neutralizing sera from individuals after recovering from SARS-CoV-2 infection, as well as from vaccinated individuals can stimulate antibody-dependent cellular cytotoxicity (ADCC), contributing to the effectiveness of vaccines [41–43]. In addition, non-neutralizing Abs induced by SARS-CoV-2 infection or COVID-19 vaccines have been associated with protection against Omicron variants via Fc-mediated non-neutralizing effector functions [44,45]. The vaccine effectiveness produced against the SARS-CoV-2 ancestral virus remains high for preventing severe disease and hospitalization caused by VOCs such as Omicron. This protection is probably mediated, at least in part, by the effector functions of Fc-dependent antibodies, in addition to T cell responses against spike proteins or more conserved antigens [39]. Serum transfer experiments from mice immunized with SpiN-Tec showed that antibodies, although non-neutralizing, partially protect the lungs against challenge with the Omicron variant. Therefore, our studies corroborate previous findings suggesting that non-neutralizing Abs may contribute to protection from severe disease, even if they cannot prevent infection. However, we did not investigate the role of the Fc portion, which may exert effector functions of non-neutralizing antibodies, contributing to immunity to SARS-CoV-2. Importantly, another study showed that antibodies from COVID-19 patients against the N protein and S protein RBD domains could stimulate high levels of ADCC response, which may support our RDB and N protein-based vaccine [46].

In parallel the role of T cells in protection against the Omicron variant was suggested by the increased number of $CD4^+$ and $CD8^+$ T cells producing IFN-γ and $CD8^+$ T cells producing Granzyme B in K18-hACE2 mice vaccinated with SpiN-Tec and challenged with Omicron. Animals depleted of $CD4^+$ and $CD8^+$ T cells showed a significantly higher viral load in the nasal wash than those non-depleted, further suggesting the participation of T cells in controlling viral dissemination.

During the COVID-19 pandemic, vaccines based on different platforms were developed and approved for emergency use. Comparative studies between homologous and heterologous prime/boost vaccination schedules have indicated that the heterologous ChAdOx1/mRNA vaccine (ChAdOx1/Comirnaty or mRNA-1273) regimen is well tolerated and induces strong immune humoral and cellular response compared to one dose or two doses of ChAdOx1 [28,47–53]. Furthermore, given the emergence of SARS-CoV-2 variants, various studies have demonstrated the efficacy of the homologous/heterologous schedule ChAdOx1 vaccine against variants such as Delta or Omicron [54–56].

Here, we demonstrated that the SpiN-Tec vaccine protected K18-hACE2 mice and hamsters challenged with the Wuhan, Delta and Omicron variants from lethality and lung pathology. In addition, SpiN-Tec has been shown to be a safe and effective vaccine in tests performed in a rat model, allowing us to advance to phase I/II clinical trials. Although SpiN-Tec did not induce nAb production, heterologous immunization using priming with ChAdOx1 demonstrated that SpiN-Tec enhances the nAbs response when used as a booster dose. In addition, SpiN-Tec induced a similar T cell response by splenocytes stimulated with recombinant RBD and SpiN, compared to ChAdOx1, indicating that SpiN-Tec is a potential vaccine candidate to be used as a booster.

Overall, this preclinical study carried out in mouse, hamster, and rat models provides consistent data on the safety, immunogenicity, and efficacy of the SpiN-Tec vaccine for the wild-type strain (Wuhan), and Delta and Omicron variants, further highlighting the importance of the T cell-mediated immune response, in addition to specific non-neutralizing Abs, in protecting against severe disease that may be caused by new circulating variants.

Data and materials availability

All data are available in the main text or the supplementary materials.

Competing interests

RTG, APF, SRT, FF, JTC, NS, NSH-S, GGR, POA and FFB are co-inventors of the potential COVID-19 vaccine evaluated in this study. The patent is under evaluation process, application number BR1020210095733. The other authors declare no competing interests.

Supplementary data to this article can be found online at https://doi.org/10.1016/j.vaccine.2024.126394.

CRediT authorship contribution statement

Natália S. Hojo-Souza: Writing – review & editing, Writing – original draft, Visualization, Methodology, Investigation, Formal analysis, Data curation, Conceptualization. **Júlia T. de Castro:** Visualization, Methodology, Investigation, Formal analysis, Data curation, Conceptualization. **Graziella G. Rivelli:** Methodology, Investigation, Formal analysis. **Patrick O. Azevedo:** Writing – review & editing, Writing – original draft, Visualization, Methodology, Investigation, Formal analysis, Conceptualization. **Emiliano R. Oliveira:** Investigation. **Lídia P. Faustino:** Investigation. **Natália Salazar:** Methodology, Investigation, Conceptualization. **Flávia F. Bagno:** Methodology, Investigation. **Alex F. Carvalho:** Methodology, Investigation. **Karine L. Lourenço:** Investigation. **Isabela P. Gomes:** Investigation. **Bruna R.D. Assis:** Investigation. **Mariela Piccin:** Investigation. **Flávio G. Fonseca:** Methodology, Conceptualization. **Edison Durigon:** Methodology. **João S. Silva:** Methodology, Funding acquisition. **Renan P. de Souza:** Methodology. **Gisele A.C. Goulart:** Methodology, Conceptualization. **Helton Santiago:** Writing – review & editing, Conceptualization. **Ana Paula S. Fernandes:** Funding acquisition, Conceptualization. **Santuza R. Teixeira:** Writing – review & editing, Funding acquisition, Conceptualization. **Ricardo T. Gazzinelli:** Writing – review & editing, Writing – original draft, Visualization, Supervision, Project administration, Methodology, Funding acquisition, Data curation, Conceptualization.

Declaration of competing interest

The authors declare the following financial interests/personal relationships which may be considered as potential competing interests: Ricardo Tostes Gazzinelli reports financial support was provided by Rede Virus from the Ministry of Science, Technology and Innovation. Ricardo Tostes Gazzinelli reports financial support was provided by National Council for Scientific and Technological Development. Ricardo Tostes Gazzinelli reports financial support was provided by National Institute of Science and Technology of Vaccines. Ricardo Tostes Gazzinelli reports financial support was provided by State of São Paulo Research Foundation. Ricardo Tostes Gazzinelli reports financial

support was provided by Ministry of Education. Ricardo Tostes Gazzinelli reports financial support was provided by Oswaldo Cruz Foundation. Ricardo Tostes Gazzinelli reports financial support was provided by Belo Horizonte City Council. Ricardo Tostes Gazzinelli reports financial support was provided by Parliamentary Amendment of State and Federal Representatives from Minas Gerais. Ricardo Tostes Gazzinelli has patent #BR1020210095733 issued to Licensee. If there are other authors, they declare that they have no known competing financial interests or personal relationships that could have appeared to influence the work reported in this paper.

Data availability

Data will be made available on request.

Acknowledgments

This work is a tribute to the memory of Dr. Alexandre de Magalhães Vieira Machado. We thank the NB3 laboratory from Faculdade de Medicina - USP and from Instituto de Ciências Biológicas – UFMG. This work was funded by Rede Virus from the Ministry of Science, Technology and Innovation, (Finep 01.20.0010 and 01.20.0005.00; CNPq 403514/2020-7 and 403701/2020-1 R.T.G.); National Institute of Science and Technology of Vaccines (Fapemig APQ-03608-17/CNPq 465293/2014-0 R.T.G.); FAPESP (2020/05527-0 R.T.G.); Ministry of Education (CAPES); Fundação Oswaldo Cruz (INOVA, 2020), Prefeitura de Belo Horizonte; as well as Parliamentary Amendment of State and Federal Representatives from Minas Gerais.

References

[1] Oronsky B, Larson C, Caroen S, Hedjran F, Sanchez A, Prokopenko E, et al. Nucleocapsid as a next-generation COVID-19 vaccine candidate. Int J Infect Dis 2022;122:529–30. https://doi.org/10.1016/j.ijid.2022.06.046.
[2] Castro JT, Azevedo P, Fumagalli MJ, Hojo-Souza NS, Salazar N, Almeida GG, et al. Promotion of neutralizing antibody-independent immunity to wild-type and SARS-CoV-2 variants of concern using an RBD-Nucleocapsid fusion protein. Nat Commun 2022;13:4831. https://doi.org/10.1038/s41467-022-32547-y.
[3] Goel RR, Painter MM, Apostolidis SA, Mathew D, Meng W, Rosenfeld AM, et al. mRNA vaccines induce durable immune memory to SARS-CoV-2 and variants of concern. Science 2021;374:abm0829. https://doi.org/10.1126/science.abm0829.
[4] Tarke A, Coelho CH, Zhang Z, Dan JM, Yu ED, Methot N, et al. SARS-CoV-2 vaccination induces immunological T cell memory able to cross-recognize variants from alpha to omicron. Cell 2022;185(5):847–859.e11. https://doi.org/10.1016/j.cell.2022.01.015.
[5] Keeton R, Tincho MB, Ngomti A, Baguma R, Benede N, Suzuki A, et al. T cell responses to SARS-CoV-2 spike cross-recognize Omicron. Nature 2022;603(7901):488–92. https://doi.org/10.1038/s41586-022-04460-3.
[6] GeurtsvanKessel CH, Geers D, Schmitz KS, Mykytyn AZ, Lamers MM, Bogers S, et al. Divergent SARS-CoV-2 omicron–reactive T and B cell responses in COVID-19 vaccine recipients. Sci immunol 2022;7:eabo2202. https://doi.org/10.1126/sciimmunol.abo2202.
[7] Gao Y, Cai C, Grifoni A, Müller TR, Niessl J, Olofsson A, et al. Ancestral SARS-CoV-2-specific T cells cross-recognize the omicron variant. Nat Med 2022;28:472–6. https://doi.org/10.1038/s41591-022-01700-x.
[8] Geers D, Shamier MC, Bogers S, Hartog GD, Gommers L, Nieuwkoop NN, et al. SARS-CoV-2 variants of concern partially escape humoral but not T-cell responses in COVID-19 convalescent donors and vaccines. Sci Immunol 2021;6:eabj1750. https://doi.org/10.1126/sciimmunol.abj1750.
[9] Dangi T, Class J, Palacio N, Richner JM, Penaloza MacMaster P. Combining spike- and nucleocapsid-based vaccines improves distal control of SARS-CoV-2. Cell Rep 2021;36(10):109664. https://doi.org/10.1016/j.celrep.2021.109664.
[10] Hong SH, Oh H, Park YW, Kwak HW, Oh EY, Park HJ, et al. Immunization with RBD-P2 and N protects against SARS-CoV-2 in nonhuman primates. Sci Adv 2021;7(22):eabg7156. https://doi.org/10.1126/sciadv.abg7156.
[11] Clemens SAC, Weckx L, Clemens R, Mendes AVA, Souza AR, Silveira MBV, et al. Heterologous versus homologous COVID-19 booster vaccination in previous recipients of two doses of CoronaVac COVID-19 vaccine in Brazil (RHH-001): a phase 4, non-inferiority, single blind, randomised study. Lancet 2022;399:521–9. https://doi.org/10.1016/S0140-6736(22)00094-0.
[12] Zuo F, Abolhassani H, Du L, Piralla A, Bertoglio F, Campos-Mata L. Heterologous immunization with inactivated vaccine followed by mRNA-booster elicits strong immunity against SARS-CoV-2 omicron variant. Nat Commun 2022;13:1–8. https://doi.org/10.1038/s41467-022-30340-5.
[13] Dias Assis BR, Gomes IP, Castro JT, Rivelli GG, Castro NS, Gomez-Mendoza DP, et al. Quality attributes of CTVad1, a nanoemulsified adjuvant for phase I clinical trial of SpiN COVID-19 vaccine. Nanomedicine 2023;18(18):1175–94. https://doi.org/10.2217/nnm-2023-0122.
[14] Frey A, Di Canzio J, Zurakowski D. A statistically defined endpoint titer determination method for immunoassays. J Immunol Methods 1998;221(1–2):35–41. https://doi.org/10.1016/s0022-1759(98)00170-7.
[15] Azevedo PO, Hojo-Souza NS, Faustino LP, Fumagalli MJ, Hirako IC, Oliveira ER, et al. Differential requirement of neutralizing antibodies and T cells on protective immunity to SARS-CoV-2 variants of concern. NPJ Vaccines 2023;8(1):15. https://doi.org/10.1038/s41541-023-00616-y.
[16] Sharp P, Villano JS. The laboratory rat. 2nd ed. CRC press; 2012.
[17] Delwatta SL, Gunatilake M, Baumans V, Seneviratne MD, Dissanayaka ML, Batagoda SS, et al. Reference values for selected hematological, biochemical and physiological parameters of Sprague-Dawley rats at the animal house, Faculty of Medicine, University of Colombo. Sri Lanka Anim Model Exp Med 2018;1:250–4. https://doi.org/10.1002/ame2.12041.
[18] Takahashi S, Hirai N, Shirai M, Ito K, Asai F. Comparison of the blood coagulation profiles of ferrets and rats. J Vet Med Sci 2011;73:953–6. https://doi.org/10.1292/jvms.10-0489.
[19] Chan JF, Zhang AJ, Yuan S, Poon VK, Chan CC, Lee AC, et al. Simulation of the clinical and pathological manifestations of coronavirus disease 2019 (COVID-19) in a Golden Syrian Hamster model: implications for disease pathogenesis and transmissibility. Clin Infect Dis 2020;71(9):2428–46. https://doi.org/10.1093/cid/ciaa325.
[20] Sia SF, Yan LM, Chin AWH, Fung K, Choy KT, Wong AYL, et al. Pathogenesis and transmission of SARS-CoV-2 in golden hamsters. Nature 2020;583(7818):834–8. https://doi.org/10.1038/s41586-020-2342-5.
[21] WHO. Coronavirus (COVID-19) Dashboard. https://covid19.who.int/table; 2024. Accessed: May 2024.
[22] Zhang Z, Shen Q, Chang H. Vaccines for COVID-19: a systematic review of immunogenicity, current development, and future prospects. Front Immunol 2022;13:843928. https://doi.org/10.3389/fimmu.2022.843928.
[23] Carabelli AM, Peacock TP, Thorne LG, Harvey WT, Hughes J. COVID-19 genomics UK consortium, *et al.* SARS-CoV-2 variant biology: immune escape, transmission and fitness. Nat Rev Microbiol 2023;21:162–77. https://doi.org/10.1038/s41579-022-00841-7.
[24] Naranbhai V, Nathan A, Kaseke C, Berrios C, Khatri A, Choi S, et al. T cell reactivity to the SARS-CoV-2 omicron variant is preserved in most but not all individuals. Cell 2022;185:1041–51. https://doi.org/10.1016/j.cell.2022.01.029.
[25] Liu J, Chandrashekar A, Sellers D, Barrett J, Jacob-Dolan C, Lifton M, et al. Vaccines elicit highly conserved cellular immunity to SARS-CoV-2 omicron. Nature 2022;603:493–6. https://doi.org/10.1038/s41586-022-04465-y.
[26] Grifoni A, Weiskopf D, Ramirez SI, Mateus J, Dan JM, Moderbacher CR, et al. Targets of T cell responses to SARS-CoV-2 coronavirus in humans with COVID-19 disease and unexposed individuals. Cell 2020;181:01–1489. https://doi.org/10.1016/j.cell.2020.05.015.
[27] Tarke A, Sidney J, Kidd CK, Dan JM, Ramirez SI, Yu ED, et al. Comprehensive analysis of T cell immunodominance and immunoprevalence of SARS-CoV-2 epitopes in COVID-19 cases. Cell Rep 2021;2:100204. https://doi.org/10.1016/j.xcrm.2021.100204.
[28] Nelde A, Bilich T, Heitmann JS, Maringer Y, Salih HR, Roerden M, et al. SARS-CoV-2-derived peptides define heterologous and COVID-19-induced T cell recognition. Nat Immunol 2020;22:74–85. https://doi.org/10.1038/s41590-020-00808-x.
[29] López-Muñoz AD, Kosik I, Holly J, Yewdell JW. Cell surface SARS-CoV-2 nucleocapsid protein modulates innate and adaptive immunity. Sci Adv 2022;8:eabp9770. https://doi.org/10.1126/sciadv.abp9770.
[30] Ahlén G, Frelin L, Nikouyan N, Weber F, Höglund U, Larsson O, et al. The SARS-CoV-2 N protein is a good component in a vaccine. J Virol 2020;94:20–e01279. https://doi.org/10.1128/jvi.01279-20.
[31] Feng W, Xiang Y, Wu L, Chen Z, Li Q, Chen J, et al. Nucleocapsid protein of SARS-CoV-2 is a potential target for developing new generation of vaccine. J Clin Lab Anal 2022;36:e24479. https://doi.org/10.1002/jcla.24479.
[32] Wu W, Cheng Y, Zhou H, Sun C, Zhang S. The SARS-CoV-2 nucleocapsid protein: its role in the viral life cycle, structure and functions, and use as a potential target in the development of vaccines and diagnostics. Virol J 2023;20:1–16. https://doi.org/10.1186/s12985-023-01968-6.
[33] Peng Y, Mentzer AJ, Liu G, Yao X, Yin Z, Dong D, et al. Broad and strong memory CD4+ and CD8+ T cells induced by SARS-CoV-2 in UK convalescent individuals following COVID-19. Nat Immunol 2020;21:1336–45. https://doi.org/10.1038/s41590-020-0782-6.
[34] Yu H, Guan F, Miller H, Lei J, Liu C. The role of SARS-CoV-2 nucleocapsid protein in antiviral immunity and vaccine development. Emerg Microbes & infect 2023;12:e2164219. https://doi.org/10.1080/22221751.2022.2164219.
[35] Addetia A, Piccoli L, Case JB, Park YJ, Beltramello M, Guarino B, et al. Neutralization, effector function and immune imprinting of omicron variants. Nat 2023;621:592–601. https://doi.org/10.1038/s41586-023-06487-6.
[36] Hajnik RL, Plante JA, Liang Y, Alameh MG, Tang J, Bonam SR, et al. Dual spike and nucleocapsid mRNA vaccination confer protection against SARS-CoV-2 omicron and Delta variants in preclinical models. Sci Transl Med 2022;14:eabq1945. https://doi.org/10.1126/scitranslmed.abq1945.
[37] O'Hagan DT, Ott GS, Nest GV, Rappuoli R, Giudice GD. The history of MF59® adjuvant: a phoenix that arose from the ashes. Expert Rev Vaccines 2013;12:13–30. https://doi.org/10.1586/erv.12.140.
[38] Knudsen NPH, Olsen A, Buonsanti C, Follmann F, Zhang Y, Coler RN, et al. Different human vaccine adjuvants promote distinct antigen-independent immunological signatures tailored to different pathogens. Sci Rep 2016;6:19570. https://doi.org/10.1038/srep19570.

[39] Zhang A, Stacey HD, D'Agostino MR, Tugg Y, Marzok A, Miller MS. Beyond neutralization: fc-dependent antibody effector functions in SARS-CoV-2 infection. Nat Rev Immunol 2023;23:381–96. https://doi.org/10.1038/s41577-022-00813-1.
[40] Beaudoin-Bussières G, Chen Y, Ullah I, Prévost J, Tolbert WD, Symmes K, et al. A fc-enhanced NTD-binding non-neutralizing antibody delays virus spread and synergizes with a nAb to protect mice from lethal SARS-CoV-2 infection. Cell Rep 2022;38:110368. https://doi.org/10.1016/j.celrep.2022.110368.
[41] Yu Y, Wang M, Zhang X, Li S, Lu Q, Zeng H, et al. Antibody-dependent cellular cytotoxicity response to SARS-CoV-2 in COVID-19 patients. Sig Transduct Target Ther 2021;6:346. https://doi.org/10.1038/s41392-021-00759-1.
[42] Tso FY, Lidenge SJ, Poppe LK, Peña PB, Privatt SR, Bennett SJ, et al. Presence of antibody-dependent cellular cytotoxicity (ADCC) against SARS-CoV-2 in COVID-19 plasma. PLoS One 2021;16:e0247640. https://doi.org/10.1371/journal.pone.0247640.
[43] Hagemann K, Riecken K, Jung JM, Hildebrandt H, Menzel S, Bunders MJ, et al. Natural killer cell-mediated ADCC in SARS-CoV-2-infected individuals and vaccine recipients. Eur J Immunol 2022;52:1297–307. https://doi.org/10.1002/eji.202149470.
[44] Bates TA, Lu P, Kang YJ, Schoen D, Thornton M, McBride SK, et al. BNT162b2-induced neutralizing and non-neutralizing antibody functions against SARS-CoV-2 diminish with age. Cell Rep 2022;41:111544. https://doi.org/10.1016/j.celrep.2022.111544.
[45] Richardson SI, Madzorera VS, Spencer H, Manamela NP, van der Mescht MA, Lambson BE, et al. SARS-CoV-2 omicron triggers cross-reactive neutralization and fc effector functions in previously vaccinated, but not unvaccinated, individuals. Cell Host Microbe 2022;30:880–6. https://doi.org/10.1016/j.chom.2022.03.029.
[46] Cui T, Huang M, Su X, Lin Z, Zhong J, Yang X, et al. Potential of antibody-dependent cellular cytotoxicity in acute and recovery phases of SARS-CoV-2 infection. Infect Dis Immun 2022;2:74–82. https://doi.org/10.1002/jmv.29638.
[47] Borobia AM, Carcas AJ, Pérez-Olmeda M, Castaño L, Bertran MJ, García-Pérez J, et al. Immunogenicity and reactogenicity of BNT162b2 booster in ChAdOx1-S-primed participants (CombiVacS): a multicentre, open-label, randomised, controlled, phase 2 trial. Lancet 2021;398(10295):121–30. https://doi.org/10.1016/S0140-6736(21)01420-3.
[48] Schmidt T, Klemis V, Schub D, Mihm J, Hielscher F, Marx S, et al. Immunogenicity and reactogenicity of heterologous ChAdOx1 nCoV-19/mRNA vaccination. Nat Med 2021;27(9):1530–5. https://doi.org/10.1038/s41591-021-01464-w.
[49] Hillus D, Schwarz T, Tober-Lau P, Vanshylla K, Hastor H, Thibeault C, et al. Safety, reactogenicity, and immunogenicity of homologous and heterologous prime-boost immunisation with ChAdOx1 nCoV-19 and BNT162b2: a prospective cohort study. Lancet Respir Med 2021;9(11):1255–65. https://doi.org/10.1016/S2213-2600(21)00357-X.
[50] Hermosilla E, Coma E, Xie J, Feng S, Cabezas C, Méndez-Boo L, et al. Comparative effectiveness and safety of homologous two-dose ChAdOx1 versus heterologous vaccination with ChAdOx1 and BNT162b2. Nat Commun 2022;13(1):1639. https://doi.org/10.1038/s41467-022-29301-9.
[51] Klemis V, Schmidt T, Schub D, Mihm J, Marx S, Abu-Omar A, et al. Comparative immunogenicity and reactogenicity of heterologous ChAdOx1-nCoV-19-priming and BNT162b2 or mRNA-1273-boosting with homologous COVID-19 vaccine regimens. Nat Commun 2022;13(1):4710. https://doi.org/10.1038/s41467-022-32321-0.
[52] Vogel E, Kocher K, Priller A, Cheng CC, Steininger P, Liao BH, et al. Dynamics of humoral and cellular immune responses after homologous and heterologous SARS-CoV-2 vaccination with ChAdOx1 nCoV-19 and BNT162b2. EBioMedicine 2022;85:104294. https://doi.org/10.1016/j.ebiom.2022.104294.
[53] Bae S, Ko JH, Choi JY, Park WJ, Lim SY, Ahn JY, et al. Heterologous ChAdOx1 and Bnt162b2 vaccination induces strong neutralizing antibody responses against SARS-CoV-2 including delta variant with tolerable reactogenicity. Clin Microbiol Infect 2022;28(10):1390.e1–7. https://doi.org/10.1016/j.cmi.2022.04.019.
[54] Groß R, Zanoni M, Seidel A, Conzelmann C, Gilg A, Krnavek D, et al. Heterologous ChAdOx1 nCoV-19 and BNT162b2 prime-boost vaccination elicits potent neutralizing antibody responses and T cell reactivity against prevalent SARS-CoV-2 variants. EBioMedicine 2022;75:103761. https://doi.org/10.1016/j.ebiom.2021.103761.
[55] Shen CF, Fu YC, Ho TS, Chen PL, Lee NY, Tsai BY, et al. Pre-existing humoral immunity and $CD4^+$ T cell response correlate with cross-reactivity against SARS-CoV-2 omicron subvariants after heterologous prime-boost vaccination. Clin Immunol 2023;251:109342. https://doi.org/10.1016/j.clim.2023.109342.
[56] Yoo J, Kim Y, Mi Cha Y, Lee J, Jeong YJ, Kim SH, et al. Heterologous vaccination (ChAdOx1 and BNT162b2) induces a better immune response against the omicron variant than homologous vaccination. J Infect Public Health 2023;16(10):1537–43. https://doi.org/10.1016/j.jiph.2023.07.017.